Fungal chromatin mapping identifies BasR, as the regulatory node of bacteria-induced fungal secondary metabolism

Juliane Fischer[a,b#], Sebastian Y. Müller[c,*#], Tina Netzker[a#], Nils Jäger[d#], Agnieszka Gacek-Matthews[e,f], Kirstin Scherlach[g], Maria C. Stroe[a,b], María García-Altares[g], Francesco Pezzini[c**], Hanno Schoeler[a,b], Michael Reichelt[h], Jonathan Gershenzon[h], Mario K. C. Krespach[a,b], Ekaterina Shelest[c**], Volker Schroeckh[a], Vito Valiante[i], Thorsten Heinzel[f], Christian Hertweck[g,j], Joseph Strauss[e,+] and Axel A. Brakhage[a, b,+]

[a]Department of Molecular and Applied Microbiology, Leibniz Institute for Natural Product Research and Infection Biology (HKI), Beutenbergstrasse 11a, 07745 Jena, Germany

[b]Institute of Microbiology, Friedrich Schiller University Jena, Jena, Germany

[c]Systems Biology and Bioinformatics, HKI, Jena, Germany

[d]Department of Biochemistry, Friedrich Schiller University Jena, Jena, Germany

[e]Department for Applied Genetics and Cell Biology, BOKU-University of Natural Resources and Life Sciences, Campus Tulln , Konrad Lorenz Straße 24, A-3430 Tulln/Donau, Austria

[f]Institute of Microbiology, University of Veterinary Medicine Vienna, Veterinärplatz 1, A-1210 Vienna, Austria

[g]Department of Biomolecular Chemistry, HKI, Jena

[h]Department of Biochemistry, MPI for Chemical Ecology, Hans-Knöll-Str. 8, 07745 Jena, Germany

[i]Leibniz Research Group – Biobricks of Microbial Natural Product Syntheses, HKI, Jena, Germany

[j]Chair for Natural Product Chemistry, Friedrich Schiller University Jena, Jena, Germany

[#]equal contribution

Footnotes:

*current address: Department of Plant Sciences, University of Cambridge, Downing Street, Cambridge CB2 3EA, UK

**current address: Bioinformatics Unit, German Centre for Integrative Biodiversity Research (iDiv), Deutscher Platz 5e, 04103 Leipzig, Germany

+corresponding authors

Axel A. Brakhage	Joseph Strauss
Phone: +49 (0)3641-532 1001	Phone: +43 (0)147654-94120
Fax: +49 (0)3641-532 0802	Fax: +43 (0)136006-6392
Email: axel.brakhage@leibniz-hki.de	Email: joseph.strauss@boku.ac.at

Short title: Bacteria-induced fungal chromatin remodeling

Key words: genome-wide dual ChIP-seq, histone modification, secondary metabolism, *Aspergillus nidulans*, cross-pathway control, *Streptomyces rapamycinicus*, transcription factors, myb-like BasR, microbial interaction

Abstract

The eukaryotic epigenetic machinery is targeted by bacteria to reprogram the response of eukaryotes during their interaction with microorganisms. In line, we discovered that the bacterium *Streptomyces rapamycinicus* triggered increased chromatin acetylation and thus activation of the silent secondary metabolism *ors* gene cluster leading to the production of orsellinic acid in the fungus *Aspergillus nidulans*. Using this model we aim at understanding molecular mechanisms of communication between bacteria and eukaryotic microorganisms based on bacteria-triggered chromatin modification. By genome-wide ChIP-seq analysis of acetylated histone H3 (H3K9ac, H3K14ac) we uncovered the unique chromatin landscape in *A. nidulans* upon co-cultivation with *S. rapamycinicus*. Genome-wide acetylation of H3K9 correlated with increased gene expression, whereas H3K14 appears to function in transcriptional initiation by providing a docking side for regulatory proteins. In total, histones belonging to six secondary metabolism gene clusters showed higher acetylation during co-cultivation including the *ors*, aspercryptin, cichorine, sterigmatocystin, anthrone and 2,4-dihydroxy-3-methyl-6-(2-oxopropyl)benzaldehyde gene cluster with the emericellamide cluster being the only one with reduced acetylation and expression. Differentially acetylated histones were also detected in genes involved in amino acid and nitrogen metabolism, signaling, and genes encoding transcription factors. In conjunction with LC-MS/MS and MALDI-MS imaging, molecular analyses revealed the cross-pathway control and Myb-like transcription factor BasR as regulatory nodes for transduction of the bacterial signal in the fungus. The presence of *basR* in other fungal species allowed forecasting the inducibility of *ors*-like gene clusters by *S. rapamycinicus* in these fungi, and thus their effective interaction with activation of otherwise silent gene clusters.

69 ## Introduction

70 The eukaryotic epigenetic machinery has been shown to be targeted by bacteria. For
71 example, bacteria can secrete chromatin modifiers or proteins such as methyltransferases
72 that silence chromatin of eukaryotic cells (1, 2). As an early example, we discovered that the
73 silent secondary metabolite (SM) gene cluster for orsellinic acid (*ors*) in the filamentous
74 fungus *Aspergillus nidulans* is activated upon physical interaction with the bacterium
75 *Streptomyces rapamycinicus*. The interaction of the fungus with this distinct bacterium led to
76 increased acetylation of histone H3 lysine 9 and 14 at the *ors* gene cluster and thus to its
77 activation (3-5). The lysine acetyltransferase (KAT) responsible for the acetylation and
78 activation of the *ors* gene cluster was shown to be GcnE (4).
79 Using this model we aim at understanding the molecular mechanisms of microbial
80 communication based on bacteria-triggered chromatin modification. In order to obtain a
81 holistic view on the fungal bacterial interaction that in the future might allow predicting
82 interaction partners and discovering the molecular elements involved, we developed a
83 genome-wide chromatin immunoprecipitation (ChIP)-seq analysis specifically during co-
84 cultivation. This led to the discovery of major alterations of epigenetic marks in the fungus
85 triggered by the bacterium and the identification of BasR as the key regulatory node
86 required for linking bacterial signals with the regulation of SM gene clusters.
87

88 ## Results

89 **Genome-wide profiles of H3K9 and H3K14 acetylation in *A. nidulans* change upon co-**
90 **cultivation with *S. rapamycinicus***

91 *A. nidulans* with and without *S. rapamycinicus* was analyzed by genome-wide ChiP-seq for
92 enrichment of acetylated (ac) histone H3 at lysines K9 and K14 (Fig. 1; SI Results – Details of

93 ChIP analysis). To account for reads originating from *S. rapamycinicus* we fused the genomes
94 of *A. nidulans* (8 chromosomes) and *S. rapamycinicus*. The resulting fused genome also
95 served as reference for mapping of chromatin marks (see SI Results – Details of the ChIP
96 analysis).
97 H3K14ac and H3K9ac showed a higher degree of variability across the genome compared to
98 H3 implying a more specific regulatory dynamics by histone acetylation than through H3
99 localization. Some areas such as a region in the first half on chromosome 4 were particularly
100 enriched in those marks, potentially marking distinctive chromatin domains. A domain
101 particularly enriched for H3K9ac was found around the *ors* gene cluster (Figs. 1 c & 2), thus
102 supporting our previous data (4). The coverage profiles of H3, H3K14ac and H3K9ac have
103 consistently changed in co-culture compared to monoculture as seen in Fig 1. In particular
104 the promoter region of the genes *orsD* and *orsA* showed reduced nucleosome occupancy
105 (see Fig. 1 c). This could be due to a redistribution of nucleosomes which ultimately changes
106 the distribution of histone marks. The changes of H3K14ac in Fig. 1 are therefore likely due
107 to nucleosome rearrangements towards the translation start sites (TSS) rather than
108 increased amounts of this modification. This is supported by the observation that
109 unmodified H3 was strongly depleted throughout the *ors* cluster, especially at the *orsA* and
110 *orsD* TSS.
111

112 **Co-cultivation of *A. nidulans* with *S. rapamycinicus* had a major impact on SM gene**
113 **clusters, nitrogen assimilation, signalling and mitochondrial activity**
114 We employed two strategies to determine changes of histone modification levels. The first
115 analysis was based on the finding that histone acetylation can mostly be found on histones
116 within a gene, in particular on nucleosomes +1 and +2 (6) (Fig. S1 a). We therefore counted

117 mapped reads overlapping genes for each library. This formed the basis for a quantitative
118 comparison between monocultures and co-cultures using standard read counting methods
119 for sequencing data (see methods). Throughout this study, we refer to this method as
120 differential chromatin state (DCS) analysis. The second analysis was based on a first round of
121 peak-calling and subsequent quantification of the peaks. Comparison of the generated data
122 sets showed 84 ± 1.7 % similarity. The data obtained from the gene-based DCS method
123 (Table S1) were used for both further analyses and comparison of the culture conditions
124 using a false discovery rate (FDR) cut-off of 0.01. This does not include further filtering on
125 the log-fold changes (LFCs) to capture possible biological relevance of the detected changes.
126 Quality and absence of possible biases introduced by the co-culture or other sources were
127 further investigated by MA plots. They showed a symmetrical and even distribution around
128 LFC = 0, meeting the requirements for the statistical tests described in methods (Fig. S2).
129 DCS analysis of H3, as a proxy for nucleosome occupancy, was found to be lower (FDR <
130 0.01) in 37 genes and higher in 2 genes during co-cultivation. Using the same cut-off, during
131 bacterial-fungal co-cultivation H3K14ac levels were found to be lower for 154 genes and
132 higher for 104 genes. Differential acetylation of chromatin was found for H3K9ac with 297
133 genes with lower and 593 with significantly higher acetylation (Table S1).
134 The analysis of microarray data obtained under identical conditions showed a positive
135 correlation of higher gene expression with H3K9 acetylation (r=0.2 for all genes and r=0.5 for
136 a subset of genes showing differential acetylation; Figs. S3 & S4). Data for selected genes are
137 summarized in Table S2 showing the LFCs of H3K9ac ChIP-seq data with their corresponding
138 microarray data. In total, histones belonging to six SM gene clusters showed higher
139 acetylation during co-cultivation including the *ors*, aspercryptin, cichorine, sterigmatocystin
140 (*stc*), anthrone (*mdp*) and 2,4-dihydroxy-3-methyl-6-(2-oxopropyl)benzaldehyde (DHMBA)

141 gene cluster with the emericellamide (*eas*) cluster being the only one with reduced
142 acetylation and expression (Table S2, section V). With a few exceptions genes covered by
143 histone H3 with higher acetylation are involved in calcium signaling and asexual
144 development (Table S2, sections III & IV; Fig S5).
145 A major group of genes with lower acetylation in mixed cultivation compared to the
146 monoculture of *A. nidulans* is linked to the fungal nitrogen metabolism (Table S2, section I)
147 including genes for the utilization of primary and secondary nitrogen sources such as genes
148 of the nitrate assimilation gene cluster and the glutamine dehydrogenase gene (Figs. S6 & 3
149 a). These data were confirmed by quantifying the expression of identified genes by qRT-PCR
150 (Fig. 3 b).
151 Genes assigned to mitochondrial function showed decreased acetylation of H3K9 which
152 implied reduced mitochondrial function. This assumption was confirmed by measuring the
153 respiratory activity of fungal cells. In monoculture the fungus showed a high metabolic
154 activity, which was significantly reduced during co-cultivation (Fig. 3 c).
155

156 **Bacteria induce elements of the fungal cross-pathway control**

157 To identify transcription factors involved in transducing the bacterial signal to the fungal
158 expression machinery and because a transcription factor gene is missing in the *ors* gene
159 cluster, we analyzed the 890 differentially H3K9 acetylated genes for those annotated as
160 putatively involved in transcriptional regulation. 22 putative transcription factor-encoding
161 genes fulfilled this requirement (Table S2, section VII). Most of them (18 genes) showed
162 significantly higher acetylation in co-culture, while only 4 genes had lower acetylation.
163 Among the higher acetylated genes were *cpcA*, coding for the central transcriptional
164 activator of the cross-pathway control CpcA, as well as the bZIP transcription factor gene

165 *jlbA* (*j*un-*l*ike *b*ZIP). Both genes have been shown to be highly expressed during amino acid
166 starvation in *A. nidulans* (7, 8). Additionally, a putative orthologue (*AN7174*) of the *S.*
167 *cerevisiae bas1* gene showed an increased acetylation. In yeast, together with the
168 homeodomain protein Bas2p, Bas1p is involved in the regulation of amino acid biosynthesis
169 (9, 10). Consistently, a number of genes related to amino acid metabolism showed increased
170 acetylation for H3K9 during the co-cultivation of *A. nidulans* with *S. rapamycinicus* (Table S2,
171 section II). To correlate the ChIP-seq data with expression levels of *cpcA, jlbA* and *AN7174*
172 qRT-PCR analysis was carried out, which demonstrated up-regulation of *cpcA* and *AN7174*
173 during co-cultivation (Fig. 4 a). In *S. cerevisiae* it was shown that Gcn4 (CpcA in *A. nidulans*)
174 and Bas1p share a similar DNA-binding motif and both activate the transcription of the
175 histidine biosynthesis gene *HIS7* independently from each other (9). In line of a possible
176 involvement of these transcription factors is the observation that the addition of the
177 histidine analogue 3-aminotriazole (3-AT), which is known to induce the cross-pathway
178 control (CPC) *via* amino acid starvation, led to the production of orsellinic acid in the fungal
179 monoculture (Fig. 4 b) and to an increased expression of *orsA, cpcA* and *AN7174* (Fig. 4 c).
180 To analyze a possible involvement of these genes in the bacteria-induced activation of the
181 *ors* gene cluster, the genes *cpcA* (data not shown) and *AN7174* gene (Fig. S7 a) were deleted.
182 Deletion of *cpcA* in *A. nidulans* showed no effect on the induction of the *ors* gene cluster in
183 response to *S. rapamycinicus* (data not shown), while deletion of *AN7174* resulted in a
184 significantly reduced expression of *orsA* and *orsD*, and in complete loss of orsellinic acid
185 production (Fig. 5). Therefore, *AN7174* was named *basR* and analyzed in detail.
186

187 **The transcription factor BasR is the central regulatory node of bacteria-triggered SM gene**
188 **cluster regulation**

189 Further analysis of the *A. nidulans* genome revealed a second gene (*AN8377*) encoding a
190 putative orthologue of the *S. cerevisiae bas1* gene (Figs. 6 & S8). Both genes (*basR* &
191 *AN8377*) code for Myb-like transcription factors whose function in filamentous fungi is
192 completely unknown. We compared the H3K9 acetylation and gene expression of both
193 genes upon co-cultivation. The *basR* gene showed higher H3K9 acetylation (LFC = 0.6) and
194 drastically increased transcription (LFC = 5.85) during co-cultivation compared to *AN8377*
195 (H3K9ac LFC = -0.03; Microarray LFC = 0.14). Deletion of *AN8377* (Fig. S9 a) did not affect the
196 induction of fungal orsellinic acid production upon co-cultivation (Fig. S9 b), excluding a role
197 of *AN8377* in this process.

198 In *S. cerevisiae* Bas1p needs the interaction with Bas2p for the transcriptional activation of
199 several genes required for histidine and purine biosynthesis (9). The C-terminal activation
200 and regulatory (BIRD) domain of Bas1, which was described to mediate this Bas1p-Bas2p
201 interaction (11), is missing in BasR. It is thus not surprising that in the *A. nidulans* genome we
202 did not find an orthologue for the *S. cerevisiae bas2* gene. While the addition of 3-AT to
203 monocultures of *A. nidulans* led to the production of orsellinic acid and derivatives thereof,
204 the effect of 3-AT was abolished in the *basR* deletion mutant strain (Fig. 4 b).

205 As the transcriptional activation of *HIS7* by Bas1/Bas2 upon adenine limitation in yeast
206 requires a functional Gcn5 (GcnE in *A. nidulans*) (10), we raised the question whether GcnE is
207 needed for full *basR* expression. Addition of *S. rapamycinicus* or 3-AT to the *gcnE* deletion
208 mutant led to decreased *basR* gene expression compared to the co-culture or a monoculture
209 of the wild type with 3-AT (Fig. 4 c). These data indicate that GcnE is required for *basR*

210 expression. Inspection of the *basR* mutant strain on agar plates did not reveal further
211 obvious phenotypes (data not shown).
212 To further substantiate the influence of *basR* on the *ors* gene cluster we generated a *basR*
213 overexpression strain (Fig. S7 b) by employing the inducible *tet*^{On} system (12). Addition of
214 doxycyline to the media induced *basR* expression as well as the expression of the *ors* gene
215 cluster (Fig. 5 a). However, *basR* gene expression was already detectable without
216 doxycycline addition, indicating "leakiness" of the *tet*^{On} system. Nevertheless, production of
217 orsellinic and lecanoric acid was only detected upon doxycycline addition (Fig. 5 b),
218 supporting the important role of BasR for their biosynthesis. To address the question
219 whether other SM biosyntheses are regulated by BasR we searched for other metabolites.
220 Obvious candidates were the emericellamides, as the acetylation of the corresponding gene
221 cluster was decreased during co-cultivation (Table S2). This finding was perfectly mirrored
222 when we applied MALDI-mass spectrometry (MS) imaging which showed reduced levels of
223 emericellamides in both *basR*-overproducing colonies of *A. nidulans* and in co-grown
224 colonies in contrast to colonies without the streptomycete (Fig. 5 c).

225 **The presence of BasR in fungal species allows forecasting the inducibility of *ors*-like gene**
226 **clusters by *S. rapamycinicus***

227 To address the question whether *basR* homologues exist in other fungi and whether
228 potential homologues have similar functions, we analyzed fungal genomes using BlastP.
229 Surprisingly, obvious *basR* homologues are only present in few other *Aspergillus* spp.
230 including *Aspergillus sydowii* and *Aspergillus versicolor*, but are apparently lacking in many
231 others (Fig. S8). Interestingly, except for three additional genes in both fungi a gene cluster
232 similar to the *ors* gene cluster of *A. nidulans* was also identified (Fig. 6 a). We overexpressed
233 *basR* in *A. sydowii* using the *tet*^{On} system to analyze its function (Fig. S10). LC-MS analyses

234 revealed the appearance of novel masses which were assigned to orsellinic acid derivatives
235 (Figure 6 b).
236 Finally, we addressed the question whether the presence of the *basR* gene and the *ors* gene
237 cluster allows forecasting their inducibility by *S. rapamycinicus*. As shown in Fig. 7, also co-
238 cultivation of *A. sydowii* with *S. rapamcinicus* led to the activation of the fungal *ors* gene
239 cluster, again linking BasR with bacteria-triggered induction of the production of orsellinic
240 acid derivatives.

241 ## Discussion

242 ### ***S. rapamycinicus* induces a unique chromatin landscape in *A. nidulans***

243 By genome-wide ChIP-seq analysis of acetylated histone H3 (H3K9ac, H3K14ac) and the
244 quantification of H3 we were able to uncover the chromatin landscape in the fungus *A.*
245 *nidulans* upon co-cultivation with *S. rapamycinicus*. In an attempt to characterize the general
246 distribution of nucleosomes and acetylation marks over the genome we compared the
247 intensity of chromatin states with gene density. A lower gene density was typically found in
248 heterochromatic regions such as the centromeres and telomeres creating a repressing
249 environment (13). We found reduced H3 occupancy in heterochromatic regions indicating
250 either replacement of H3 by the centromere-specific H3, CENP-A or reduced nucleosome
251 occupancy (13, 14).
252 We observed distinct peaks for H3K9ac in *A. nidulans* grown in co-culture with *S.*
253 *rapamycinicus*. One of the areas with the highest increase in H3K9ac was the *ors* gene
254 cluster, nicely confirming our previous findings (4) (Fig. 7). Furthermore, previous ChIP qRT-
255 PCR experiments indicated a distinct increase of H3K9ac inside the cluster borders, which did
256 not expand to neighboring genes (4). By contrast, the H3K14ac modification seemed to be of
257 a more global nature and not exclusively confined to specific regions such as the *ors* gene

258 cluster. These conclusions were extended here by the pattern detected in the genome-wide
259 ChIP-seq data, showing no spreading of H3K9ac to genes adjacent to the *ors* gene cluster
260 which also demonstrates the quality of the genome-wide ChIP data generated here.
261 Furthermore, these results are also consistent with our previous finding of reduced
262 expression of SM cluster genes as a consequence of the lack of H3K14 acetylation (5). In
263 contrast to H3K14ac, H3K9ac is less uniformly distributed over the genome. It only showed
264 strong enrichment at promoters of certain genes. Especially high levels of acetylation were
265 found at *orsA* and the bidirectional promoters of *orsD* and *orsE*. This observation was
266 recently confirmed by the finding that H3ac and H3K4me3 were increased at the *orsD* gene
267 only when the *ors* cluster was transcriptionally active (15).
268 We also assessed the distribution of H3K9ac and H3K14ac as well as the C-terminus of H3
269 (H3Cterm) at the TSS and translation termination sites (TTSs) (SI Results - Chromatin profiles
270 at translation start sites and translation termination sites). For H3K9, an enrichment of
271 acetylation ~500 bp downstream of the TSS as well as immediately upstream of the TSS was
272 observed. This was expected as similar results were obtained with an antibody targeting the
273 acetylated N-terminus of histone H3 in *A. nidulans* (15) and other fungi such as *S. cerevisiae*
274 and *Cryptococcus neoformans* (16, 17). Increased acetylation coincides with reduced levels
275 of H3 around the TSS, which is most likely due to a depletion of nucleosomes at the
276 promoter. The profile plots for H3K14 acetylation are similar, although not as highly
277 enriched around the TSS as H3K9 (Fig. S11 a). As expected, a comparison of LFCs for both
278 modifications showed high similarity suggesting that they are established interdependently
279 (18, 19). At the 3' end of the ORF, H3 density drastically increased accompanied by reduced
280 levels of H3K9ac and H3K14ac (Fig. S11). Likewise, reduced acetylation at the TTS was
281 observed in *A. nidulans* (15) and *S. cerevisiae* (17). It is interesting to notice, that the increase

282 in nucleosome density directly correlated with a decrease in the gene expression rate (Fig.
283 S12 e). Previous studies suggested a direct correlation between the presence of
284 nucleosomes and the stalling of RNA polymerase II (20).
285

286 **Increased gene expression directly correlates with histone H3K9 acetylation**

287 Acetylation is generally regarded as an activating chromatin mark promoting transcription of
288 eukaryotic genes (21). Our study suggests a more differentiated picture. When we compared
289 data from this study with microarray data (4) (Figs. S3 & S4) the acetylation of H3K9 directly
290 correlated with gene expression levels. A similar finding was reported for other fungi (22). By
291 contrast, this was not observed for acetylation of H3K14. This could partly result from the
292 low number of targets for this modification. By contrast, gene promoters showed a distinct
293 increase of H3K14ac at the TSS in dependence on the average transcription level (Fig. S12 c).
294 The low correlation between active gene transcription and acetylation at H3K14 confirmed
295 earlier results. Previously, we showed that a mimicry of a hypo-acetylated lysine 14 on
296 histone H3 drastically altered the phenotype and the expression of SM gene clusters in this
297 strain (5). This effect, however, was overcome when later time points of cultivation were
298 considered. Taken together, the primary location at the TSS and the major defect in SM
299 production at earlier stages indicate a role for H3K14ac in transcriptional initiation. Hyper-
300 acetylation at H3K14 could be also relevant for marking active genes and providing a docking
301 side for regulatory proteins.
302

303 ***S. rapamycinicus* silences fungal nitrogen metabolism**

304 A substantial number of genes involved in primary and secondary nitrogen metabolism were
305 strongly depleted for H3K9ac upon co-cultivation. This correlated with reduced expression of
306 the respective genes. Thus, upon contact with the bacterium, *A. nidulans* showed reduced
307 nitrogen uptake and reduced degradation of various nitrogen sources, leading to nitrogen
308 starvation.

309 Under nitrogen starvation or low availability of primary nitrogen sources, such as glutamine
310 and ammonium, the intracellular level of glutamine drops (23). This was in fact observed for
311 the intracellular concentration of amino acids in *A. nidulans* when the fungus was co-
312 cultured with the bacterium (Fig. S13). Thus, in presence of *S. rapamycinicus* but not of non-
313 inducing streptomycetes like *S. lividans* the fungus is in a physiological state of nitrogen
314 starvation (Fig. 7). Nitrogen limitation was shown before to represent a trigger for the
315 activation of a number of SM gene clusters including the *ors* gene cluster (24, 25). Nitrogen
316 starvation also activates the expression of the anthrone (*mdp*) gene cluster (24), which we
317 also observed in our data. However, induction of orsellinic acid production by nitrogen
318 starvation took about 60 h, whereas co-cultivation with *S. rapamycinicus* already triggered
319 expression of the cluster genes after 3 h. Therefore, it is unlikely that the bacteria-triggered
320 activation of the cluster is exclusively achieved by restricting nitrogen availability for the
321 fungus. Furthermore, shortage of nitrogen leads to de-repression of genes involved in the
322 usage of secondary nitrogen sources, which was not supported by our data. In *S. cerevisiae*,
323 it was shown that a shift from growth under nutrient sufficiency to nitrogen starvation
324 induced degradation of mitochondria (26). Similarly, upon contact of *A. nidulans* with the
325 bacterium decreased acetylation and transcription of genes with mitochondrial function

326 were also detected. This was further supported by a lower mitochondrial respiratory activity
327 in the fungal cells during co-cultivation (Fig. 3 c).
328

329 **BasR is a central regulatory node for integrating bacterial signals leading to regulation of**
330 **SM gene clusters**

331 Another consequence of nitrogen starvation is the reduced availability of amino acids in the
332 cell. Consequently, as shown here, the amino acid biosynthetic pathways represented a
333 major group of de-regulated genes at both the acetylation level and expression level. Amino
334 acid biosyntheses in fungi are regulated by the CPC system upon starvation for distinct
335 amino acids (23, 27). Since deletion of *cpcA* in *A. nidulans* did not affect the induction of the
336 *ors* gene cluster, but on the other hand the artificial inducer of the CPC system 3-AT (28), it
337 was conceivable that CPC somehow plays a role. 3-AT is a structural analogue of histidine
338 triggering histidine starvation in the fungal cell and thereby the CPC (28). In *S. cerevisiae*,
339 other regulators were also shown to induce the CPC such as the heterodimeric transcription
340 factor complex Bas1/Bas2p (10, 29) which is even bound by Gcn5. We identified two
341 putative orthologous genes in the genome of *A. nidulans*. Further analysis revealed only
342 *basR (AN7174)* as being involved in the *ors* gene cluster activation during the fungal-bacterial
343 co-cultivation (Fig. 7). Despite the fact that *AN8377* seems to be more similar to the *S.*
344 *cerevisiae bas1* (Figs. 6 & S8), it is not needed for the *ors* gene cluster activation.

345 Based on bioinformatic analysis BasR of *A. nidulans* consists of 305 amino acids and thus is
346 rather different from its closest homolog Bas1p of *S. cerevisiae* with 811 amino acids (30).
347 The BIRD region of Bas1p mediating the Bas1p-Bas2p interaction (11), is missing in BasR. The
348 *basR* gene was highly up-regulated in the microarray data which coincided with increased
349 H3K9 acetylation of its promoter. *basR* deletion and overexpression clearly demonstrated

350 the function of this transcription factor gene in activating the *ors* gene cluster in dependence
351 of *S. rapamycinicus*. For efficient *basR* expression a functional GcnE seems to be required,
352 indicating a similar dependency as observed for *bas1* in yeast (10).
353 Interestingly, the *basR* gene could not be found in all fungal genomes analyzed here, but for
354 example in *A. sydowii* and *A. versicolor* which were also found to encode *ors* gene clusters.
355 Like in *A. nidulans*, overexpression of the *A. sydowii basR* gene led to the activation of its
356 silent *ors* gene cluster. Based on this finding we predicted that *S. rapamycinicus* also induces
357 the *ors* gene cluster in *A. sydowii* which indeed was the case. We did not find a *basR*
358 homologue in *A. fumigatus* although the formation of fumicyclines is induced by *S.*
359 *rapamycinicus* (31). This might be due to the genome data available that lack the *basR* gene
360 due to missing annotation or, alternatively, a different regulatory response mechanism to *S.*
361 *rapamycinicus* is present in *A. fumigatus*.
362 Genome-wide ChIP-seq analysis also indicated that the interaction of *S. rapamycinicus* with
363 *A. nidulans* influenced other SM gene clusters, *e.g.*, it led to repression of the formation of
364 emericellamides. Also for this repression, BasR was required, indicating that overexpression
365 of *basR* phenocopies the regulation by *S. rapamycinicus*. As implied by the finding that the
366 presence of *basR* and the *ors* cluster in several fungi coincided with their inducibility by *S.*
367 *rapamycinicus*, in future it might be possible to predict which microorganisms talk to each
368 other based on their genetic inventory.

369 ## Material and Methods

370 **Microorganisms, media and cultivation.** Microorganisms are listed in Table S4. *A. nidulans*
371 strains were cultivated in *Aspergillus* minimal medium (AMM) at 37 °C, 200 rpm (32). When
372 required, supplements were added as follows: arginine (871 µg/mL), *p*-aminobenzoic acid (3
373 µg/mL) and pyridoxine HCl (5 µg/mL). Pre-cultures were inoculated with 4×10^8 spores per

374 mL. 10 µg/mL doxycycline was used to induce the *tet*^{On} inducible system. For the
375 measurement of orsellinic acid, mycelia of overnight cultures (~16 h) in AMM were
376 transferred to fresh medium and inoculated with *S. rapamycinicus*, as previously described
377 (3). RNA extraction for expression analysis during co-cultivation was performed after 3 hours
378 of cultivation, for analysis of the *basR* overexpression mutant after 6 hours of monoculture;
379 samples for HPLC analysis were taken after 24 h. *A. sydowii* was cultivated at 28 °C, 200 rpm
380 in malt medium (33). For the induction of the *ors* cluster in *A. sydowii*, 48-hour old
381 precultures were transferred to fresh AMM and inoculated with *S. rapamycinicus* or
382 doxycycline. 10 µg/mL doxycycline was added twice over the course of 48 hours. Samples
383 were taken for LC-MS analysis after 96 hours for *A. sydowii* co-cultivation and after 48 hours
384 for the *A. sydowii basR* overexpression mutant. For MALDI-MS Imaging analysis conductive
385 ITO slides (Bruker Daltonics, Bremen, Germany) were coated with 3 mL 0.5% (w/v) AMM
386 agar and incubated at room temperature for 30 minutes (34, 35). Identical conditions were
387 ensured by supplementation of all slides with arginine regardless of the fungal genotype. *S.*
388 *rapamycinicus* was applied by filling 5 mL of a preculture in a tube and point inoculation of
389 15 µl of the settled mycelium on the agar. For *A. nidulans*, 500 conidia of wild type and
390 mutants were point inoculated on the agar. For co-cultivation experiments, both
391 microorganisms were inoculated 1 cm apart from each other. The slides were incubated at
392 37 °C in a petri dish for 4 days. The slides were dried by incubation in a hybridization oven at
393 37 °C for 48 hours.
394 **Quantitative RT-PCR (qRT-PCR).** Total RNA was purified with the Universal RNA Purification
395 Kit (roboklon, Berlin, Germany). Reverse transcription of 5 µg RNA was performed with
396 RevertAid Reverse Transcriptase (Thermo Fisher Scientific, Darmstadt, Germany) for 3 hours
397 at 46 °C. qRT-PCR was performed as described before (3). The *A. nidulans* ß-actin gene

398 (*AN6542*) served as an internal standard for calculation of expression levels as previously
399 described (3). Primers for amplification of probes are listed in Table S5.

400 **Preparation of chromosomal DNA and Southern blot analysis.** *A. nidulans* genomic DNA
401 was isolated as previously described (3). Southern blotting was performed using a
402 digoxigenin-11-dUTP-labeled (Jena Bioscience, Jena, Germany) probe (3).

403 **ChIP coupled to qRT-PCR analysis.** ChIP coupled to qRT-PCR analysis including crosslinking of
404 the DNA, sonication, antibody incubation and precipitation and DNA reverse-cross-linking is
405 described in SI Material and Methods.

406 **Extraction of fungal compounds, HPLC and LC-MS analyses.** Extraction of *A. nidulans* and *A.*
407 *sydowii* monocultures as well as co-cultures with *S. rapamycinicus* and the subsequent HPLC
408 and LC-MS analysis are described in SI Material and Methods.

409 **MALDI-MS imaging analysis and data processing.** Sample preparation and matrix coating
410 were performed as previously described (34). Samples were analyzed (34) in an
411 UltrafleXtreme MALDI TOF/TOF (Bruker Daltonics, Bremen, Germany), in reflector positive
412 mode with the following modifications: 100-3000 Da range, 30 % laser intensity (laser type
413 4) and raster width 200 µm. The experiments were repeated three times (2nd and 3rd
414 replicates with 250 µm raster width). Calibration of the acquisition method, spectra
415 procession, visualization, analysis and illustration were performed as described before (34).
416 Chemical images were obtained using Median normalization and weak denoising.

417 **Resazurin assay.** Respiratory activity was measured by reduction of resazurin to the
418 fluorescent dye resorufin. 10^4 conidia of *A. nidulans* in 100 µL AMM were pipetted in each
419 well of a black 96 well plate. The plate was incubated for 16 hours at 37 °C. The pre-grown
420 fungal mycelium was further cultivated in monoculture or with 10 µL of an *S. rapamycinicus*
421 culture. Cultures were further supplemented with 100 µL of AMM containing resazurin in a

422 final concentration of 0.02 mg/mL. Fluorescence was measured (absorption wavelength 560
423 nm, emission wavelength 590 nm) every 30 minutes for 24 hours at 37 °C in a Tecan
424 Fluorometer (Infinite M200 PRO, Männedorf, Switzerland). For all conditions, measurements
425 were carried out in triplicates for each of the two biological replicates. Significance of values
426 was calculated using 2-way ANOVA Test with GraphPad Prism 5 (GraphPad Software Inc., La
427 Jolla, USA).

428 **ChIP-seq pre-processing, DCS analysis and MACS analysis** are described in SI Material and
429 Methods**.**

430 **Generation of *A. nidulans* and *A. sydwoii* mutant strains** is described in SI Material and
431 Methods.

432 **Phylogenetic analysis.** The amino acid sequences for the two Myb-like transcription factors
433 from *A. nidulans* (*AN7174* (*basR*) and *AN8377*) and Bas1 from *S. cerevisiae* were used for a
434 Blast search in the UniProtKB database. For each sequence, the first 50 hits were retrieved.
435 All hits were grouped together, and redundant and partial sequences removed. The obtained
436 54 hits were firstly aligned using MUSCLE (36). The phylogenetic tree was obtained using the
437 Maximum Likelihood method contained in the MEGA6 software facilities (37).

438 **Availability of data and materials**

439 ChIP-seq data were deposited in the ArrayExpress database at EMBL-EBI
440 (www.ebi.ac.uk/arrayexpress) under accession number E-MTAB-5819. The code for data
441 processing and analysis can be obtained from https://github.com/seb-mueller/ChIP-
442 Seq_Anidulans.

443

Acknowledgements

We thank Christina Täumer and Karin Burmeister for excellent technical assistance and Sven Krappmann (Friedrich-Alexander University, Erlangen-Nürnberg, Germany) for kindly providing plasmid pSK562. Financial support by the Deutsche Forschungsgemeinschaft (DFG)-funded excellence graduate school Jena School for Microbial Communication (JSMC), the International Leibniz Research School for Microbial and Biomolecular Interactions (ILRS) as part of the JSMC, the DFG-funded Collaborative Research Center 1127 ChemBioSys (projects B01, B02 and INF), the BMBF-funded project DrugBioTune in the frame of Infectcontrol2020 and the European Research Council for a Marie Skłodowska-Curie Individual Fellowship (IF-EF; Project reference 700036) to María García-Altares is gratefully acknowledged.

References

1. Yoshida M, Kijima M, Akita M, & Beppu T (1990) Potent and specific inhibition of mammalian histone deacetylase both in vivo and in vitro by trichostatin A. *J. Biol. Chem.* 265(28):17174-17179.
2. Rolando M*, et al.* (2013) *Legionella pneumophila* effector RomA uniquely modifies host chromatin to repress gene expression and promote intracellular bacterial replication. *Cell Host Microbe* 13(4):395-405.
3. Schroeckh V*, et al.* (2009) Intimate bacterial-fungal interaction triggers biosynthesis of archetypal polyketides in *Aspergillus nidulans*. *PNAS* 106(34):14558-14563.
4. Nützmann H-W*, et al.* (2011) Bacteria-induced natural product formation in the fungus *Aspergillus nidulans* requires Saga/Ada-mediated histone acetylation. *PNAS* 108(34):14282-14287.
5. Nützmann H-W, Fischer J, Scherlach K, Hertweck C, & Brakhage AA (2013) Distinct amino acids of histone H3 control secondary metabolism in *Aspergillus nidulans*. *Appl. Environ. Microbiol.* 79(19):6102-6109.
6. Jiang C & Pugh BF (2009) Nucleosome positioning and gene regulation: advances through genomics. *Nat. Rev. Genet.* 10(3):161-172.
7. Hoffmann B, Valerius O, Andermann M, & Braus GH (2001) Transcriptional autoregulation and inhibition of mRNA translation of amino acid regulator gene *cpcA* of filamentous fungus *Aspergillus nidulans*. *Mol. Biol. Cell* 12(9):2846-2857.
8. Strittmatter AW, Irniger S, & Braus GH (2001) Induction of *jlbA* mRNA synthesis for a putative bZIP protein of *Aspergillus nidulans* by amino acid starvation. *Curr. Genet.* 39(5-6):327-334.
9. Springer C, Künzler M, Balmelli T, & Braus GH (1996) Amino acid and adenine cross-pathway regulation act through the same 5'-TGACTC-3' motif in the yeast HIS7 promoter. *J. Biol. Chem.* 271(47):29637-29643.

480 10. Valerius O*, et al.* (2003) Nucleosome position-dependent and -independent activation of *HIS7*
481 expression in *Saccharomyces cerevisiae* by different transcriptional activators. *Eukaryot Cell*
482 2(5):876-885.
483 11. Pinson B*, et al.* (2000) Signaling through regulated transcription factor interaction: mapping
484 of a regulatory interaction domain in the Myb-related Bas1p. *Nucleic Acids Res.* 28(23):4665-
485 4673.
486 12. Helmschrott C, Sasse A, Samantaray S, Krappmann S, & Wagener J (2013) Upgrading fungal
487 gene expression on demand: improved systems for doxycycline-dependent silencing in
488 *Aspergillus fumigatus*. *Appl. Environ. Microbiol.* 79(5):1751-1754.
489 13. Allshire RC & Ekwall K (2015) Epigenetic regulation of chromatin states in
490 *Schizosaccharomyces pombe*. *Cold Spring Harbor Perspect. Biol.* 7(7):a018770.
491 14. Smith KM, Phatale PA, Sullivan CM, Pomraning KR, & Freitag M (2011) Heterochromatin is
492 required for normal distribution of *Neurospora crassa* CenH3. *Mol. Cell. Biol.* 31(12):2528-
493 2542.
494 15. Gacek-Matthews A*, et al.* (2016) KdmB, a jumonji histone H3 demethylase, regulates
495 genome-wide H3K4 trimethylation and is required for normal induction of secondary
496 metabolism in *Aspergillus nidulans*. *PLos Genet.* 12(8):e1006222.
497 16. Haynes BC*, et al.* (2011) Toward an integrated model of capsule regulation in *Cryptococcus*
498 *neoformans*. *PLoS Pathog.* 7(12):e1002411.
499 17. Mews P*, et al.* (2014) Histone methylation has dynamics distinct from those of histone
500 acetylation in cell cycle reentry from quiescence. *Mol. Cell. Biol.* 34(21):3968-3980.
501 18. Gacek A & Strauss J (2012) The chromatin code of fungal secondary metabolite gene clusters.
502 *Appl. Microbiol. Biotechnol.* 95(6):1389-1404.
503 19. Waters R, van Eijk P, & Reed S (2015) Histone modification and chromatin remodeling during
504 NER. *DNA Repair* 36:105-113.
505 20. Grosso AR, de Almeida SF, Braga J, & Carmo-Fonseca M (2012) Dynamic transitions in RNA
506 polymerase II density profiles during transcription termination. *Genome Res.* 22(8):1447-
507 1456.
508 21. Bannister AJ & Kouzarides T (2011) Regulation of chromatin by histone modifications. *Cell*
509 *Res.* 21(3):381-395.
510 22. Wiemann P*, et al.* (2013) Deciphering the cryptic genome: genome-wide analyses of the rice
511 pathogen *Fusarium fujikuroi* reveal complex regulation of secondary metabolism and novel
512 metabolites. *PLoS Pathog.* 9(6):e1003475.
513 23. Tudzynski B (2014) Nitrogen regulation of fungal secondary metabolism in fungi. *Front.*
514 *Microbiol.* 5:656.
515 24. Scherlach K*, et al.* (2011) Two induced fungal polyketide pathways converge into
516 antiproliferative spiroanthrones. *ChemBioChem* 12(12):1836-1839.
517 25. Studt L, Wiemann P, Kleigrewe K, Humpf H-U, & Tudzynski B (2012) Biosynthesis of
518 fusarubins accounts for pigmentation of *Fusarium fujikuroi* perithecia. *Appl. Environ.*
519 *Microbiol.* 78(12):4468-4480.
520 26. Eiyama A, Kondo-Okamoto N, & Okamoto K (2013) Mitochondrial degradation during
521 starvation is selective and temporally distinct from bulk autophagy in yeast. *FEBS Lett.*
522 587(12):1787-1792.
523 27. Krappmann S & Braus GH (2005) Nitrogen metabolism of *Aspergillus* and its role in
524 pathogenicity. *Med. Mycol.* 43(Supplement_1):S31-S40.
525 28. Sachs MS (1996) General and cross-pathway controls of amino acid biosynthesis.
526 *Biochemistry and Molecular Biology,* The Mycota, eds Brambl R & Marzluf GA (Springer Berlin
527 Heidelberg, Berlin, Heidelberg), Vol 3, pp 315-345.
528 29. Daignan-Fornier B & Fink GR (1992) Coregulation of purine and histidine biosynthesis by the
529 transcriptional activators BAS1 and BAS2. *PNAS* 89(15):6746-6750.

530 30. Zhang F, Kirouac M, Zhu N, Hinnebusch AG, & Rolfes RJ (1997) Evidence that complex
531 formation by Bas1p and Bas2p (Pho2p) unmasks the activation function of Bas1p in an
532 adenine-repressible step of ADE gene transcription. *Mol. Cell. Biol.* 17(6):3272-3283.
533 31. König CC*, et al.* (2013) Bacterium induces cryptic meroterpenoid pathway in the pathogenic
534 fungus *Aspergillus fumigatus*. *Chembiochem* 14(8):938-942.
535 32. Brakhage AA & Van den Brulle J (1995) Use of reporter genes to identify recessive trans-
536 acting mutations specifically involved in the regulation of *Aspergillus nidulans* penicillin
537 biosynthesis genes. *J. Bacteriol.* 177(10):2781-2788.
538 33. Scherlach K, Schuemann J, Dahse H-M, & Hertweck C (2010) Aspernidine A and B, prenylated
539 isoindolinone alkaloids from the model fungus *Aspergillus nidulans*. *J. Antibiot.* 63(7):375-
540 377.
541 34. Aiyar P*, et al.* (2017) Antagonistic bacteria disrupt calcium homeostasis and immobilize algal
542 cells. *Nat. Commun.* 8.
543 35. Araújo FDdS, Araújo WL, & Eberlin MN (2017) Potential of *Burkholderia seminalis* TC3.4.2R3
544 as biocontrol agent against *Fusarium oxysporum* evaluated by mass spectrometry imaging. *J.*
545 *Am. Soc. Mass. Spectrom.* 28(5):901-907.
546 36. Edgar RC (2004) MUSCLE: multiple sequence alignment with high accuracy and high
547 throughput. *Nucleic Acids Res.* 32(5):1792-1797.
548 37. Tamura K, Stecher G, Peterson D, Filipski A, & Kumar S (2013) MEGA6: molecular
549 evolutionary genetics analysis version 6.0. *Mol. Biol. Evol.* 30(12):2725-2729.

550

551

552 **Figures**

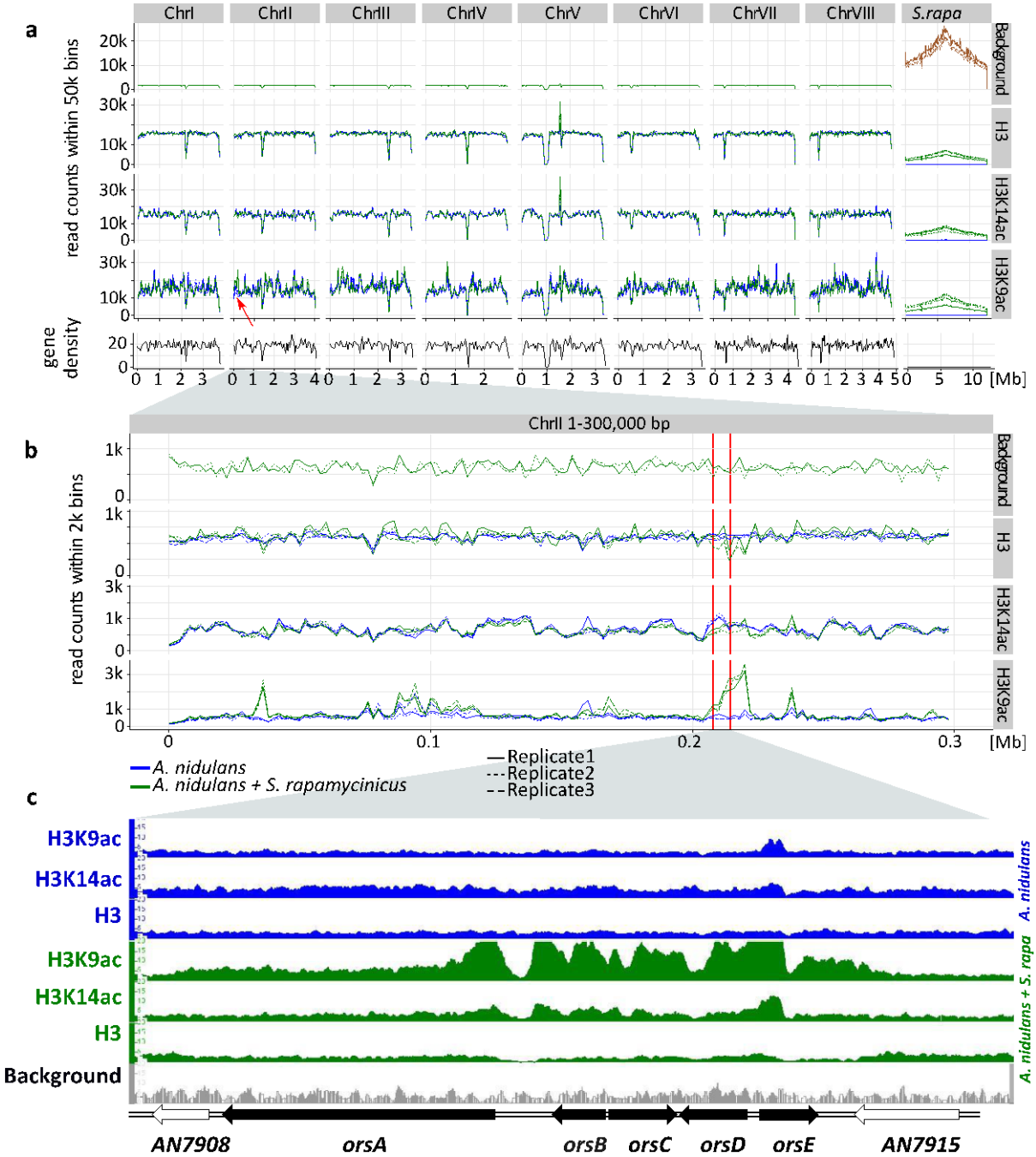

553

554 **Figure 1. Genome-wide coverage plot of the fused fungal-bacterial genome with indication**
555 **of H3(Cterm) and acetylated H3 (K9 and K14).** For each condition, ChIP-seq analyses of
556 three independent samples were performed. (**a**) Genome-wide analysis covering all
557 chromosomes. Data for all the chromosomes I to VIII of *A. nidulans* as well as for the
558 chromosome of *S. rapamycinicus* are shown. X axis corresponds to genome coordinates of
559 the fused genome in Mb. Y axis corresponds to the number of reads mapping within equally
560 sized windows (bins) which segment the fused genome at a resolution of 50 kb for each
561 library separately (see methods for details). The read count values are plotted at the

562 midpoint of each bin which then were connected by lines. Gene density is reported likewise
563 by counting the number of genes for each bin instead of reads. Background values derive
564 from *S. rapamycinicus* (brown) and *A. nidulans* (green) grown in monoculture. The red arrow
565 indicates the location of the *ors* gene cluster. (**b**) Zoom into chromosome II. The red lines
566 mark the *ors* gene cluster. Data of three replicates are shown, which show the same
567 tendency. Overall intensity of background, H3K9ac, H3K14ac and H3(Cterm) compared
568 between *A. nidulans* monoculture (blue) and co-culture (green) is shown, as well as the
569 average genome density (black). (**c**) Example of an IGV screenshot showing the region of the
570 *ors* gene cluster at the bottom of the figure labeled with black arrows. Other differentially
571 acetylated gene bodies are listed in table 1. Blank gene arrows indicate genes not belonging
572 to the *ors* gene cluster. Data obtained from monocultures of the fungus are depicted in blue,
573 from co-cultivation in green and background data in grey.
574
575

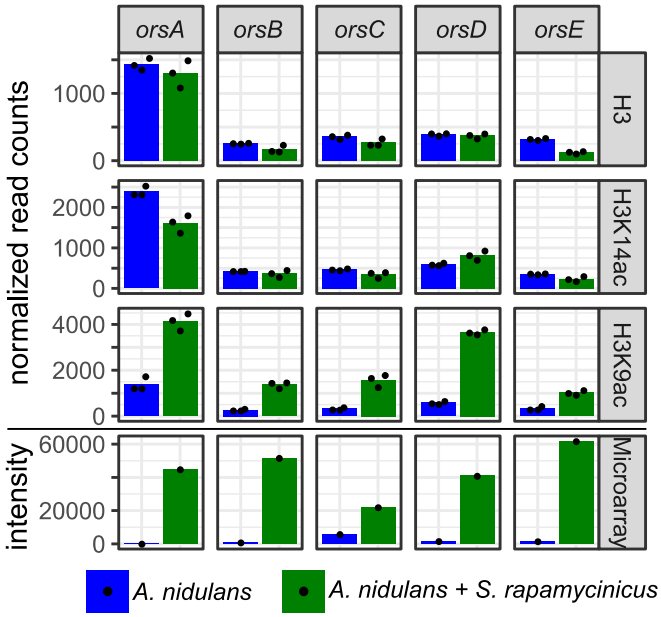

576

577 **Figure 2. Normalized read counts derived from differential chromatin state (DCS) analysis**
578 **obtained for the *ors* genes based on H3, H3K14ac and H3K9ac ChIP-seq.** Data were
579 generated for the area 500 bp down- and 1000 bp upstream from the TSS. Depicted bars are
580 calculated from three data points.

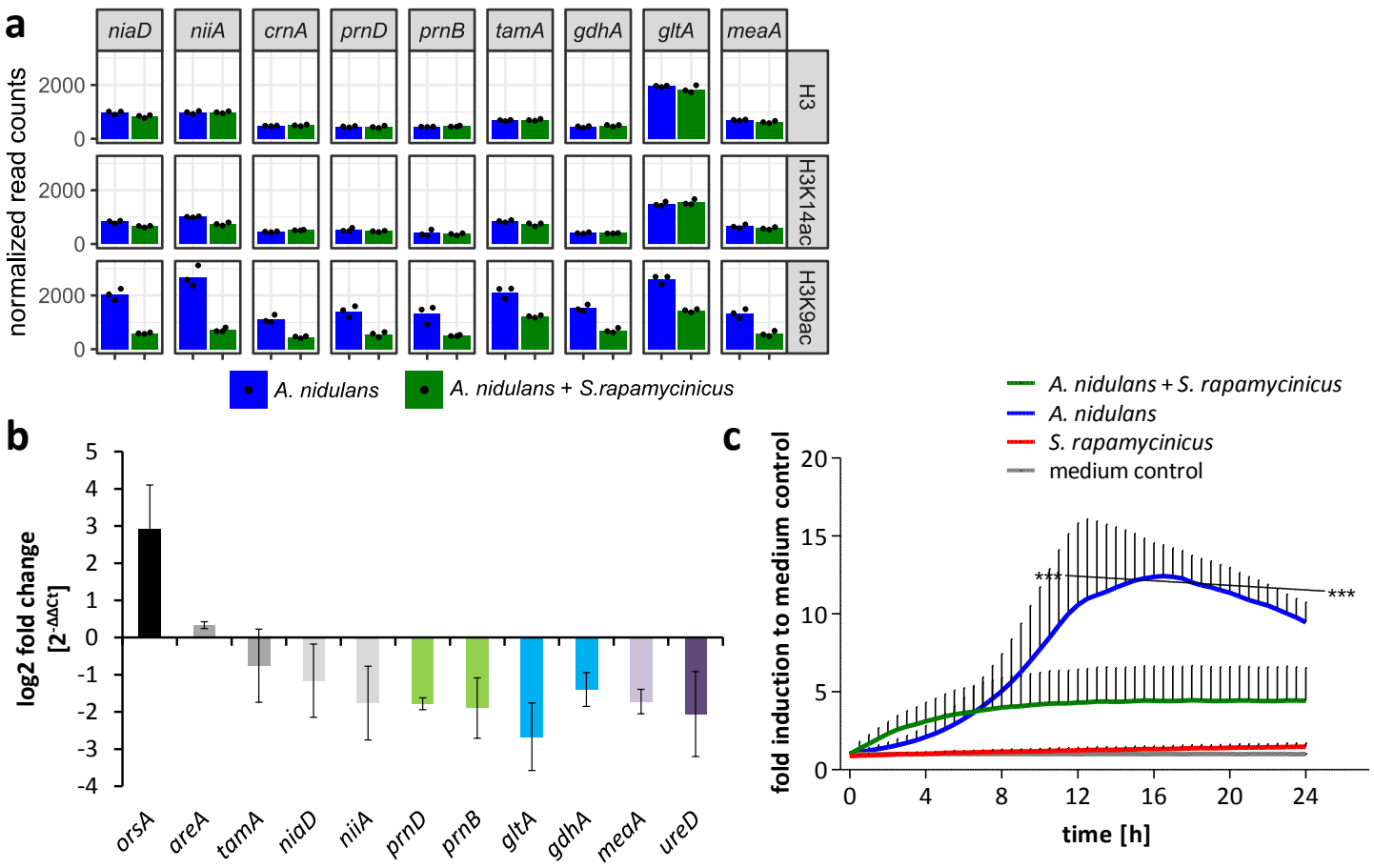

581

582 **Figure 3. Influence of *S. rapamycinicus* on the fungal nitrogen metabolism and mitochondrial functions.** (**a**) Normalized ChIP-seq read counts
583 were used to quantify chromatin state (H3, H3K14ac, H3K9ac) for nitrogen metabolism genes. Counts were obtained by counting reads mapping
584 to the promoter area for each gene that is 500 bp down- and 1000 bp upstream from the TSS. Depicted bars are calculated from three data
585 points. (**b**) Transcription analysis of randomly selected genes of primary and secondary nitrogen metabolism by qRT-PCR during co-cultivation.
586 Relative mRNA levels were measured after 3 hours and normalized to the β-actin gene expression. The transcription of *orsA* was used as a positive
587 control. (**c**) Respiratory activity comparing *A. nidulans* grown in co-culture with *S. rapamycinicus* and *A. nidulans* in monoculture. Respiratory

activity was determined using a resazurin assay. Data were normalized to medium. The black line shows the time points that are significantly different between *A. nidulans* and *A. nidulans* grown in co-culture with *S. rapamycinicus*. *** $p < 0.001$

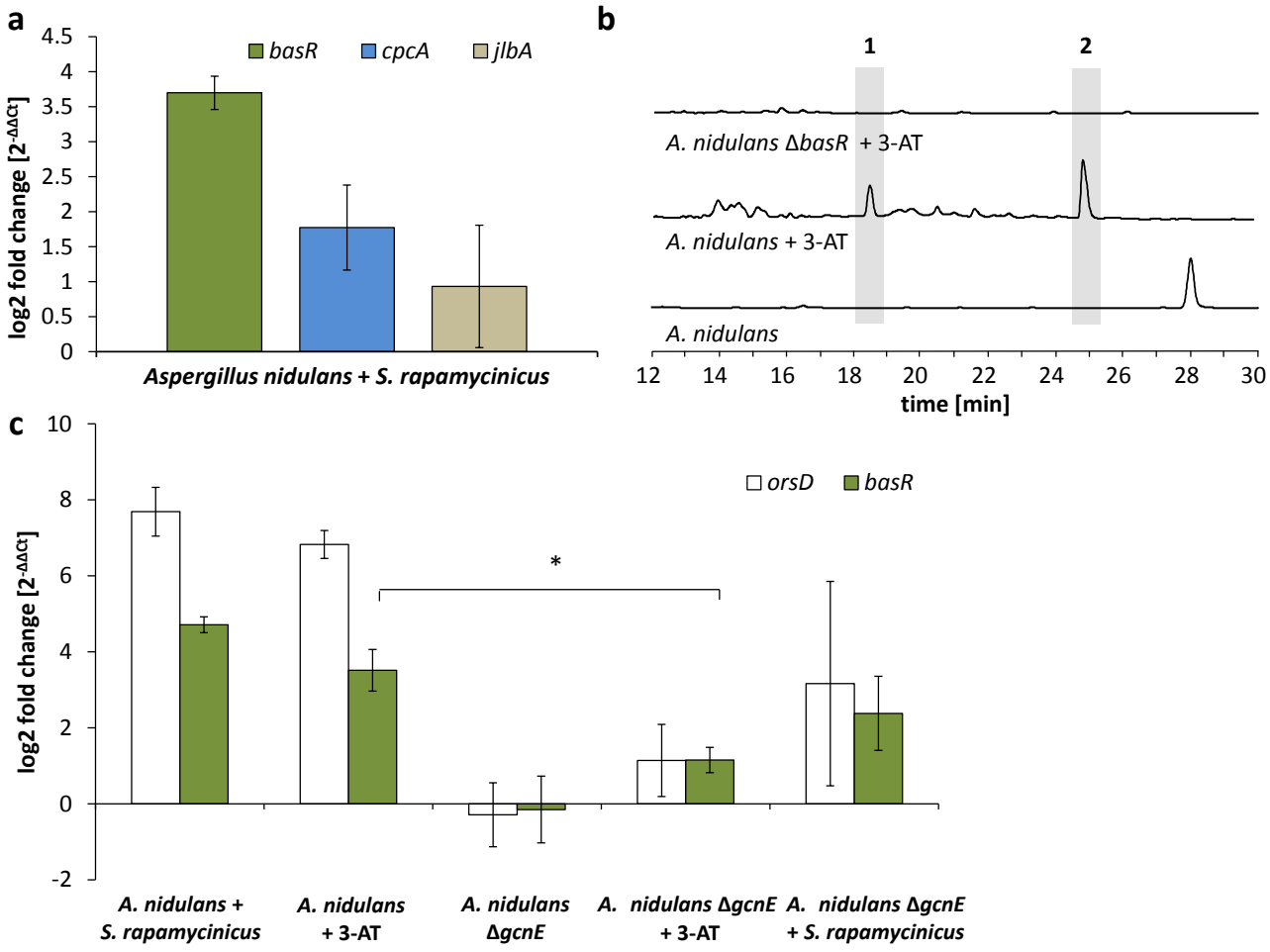

Figure 4. **Artificial histidine starvation using 3-AT led to *ors* gene cluster activation.** (**a**) Transcription of *basR, cpcA* and *jlbA* determined by qRT-PCR after 3h of co-cultivation. Relative mRNA levels were compared to β-actin gene expression. (**b**) HPLC-based detection of orsellinic acid (1) and lecanoric acid (2) in supernatants of *A. nidulans* cultures treated with 3-AT. (**c**) Relative transcript levels of *orsA*, *cpcA* and *basR* 6 hours after 3-AT addition to the *A. nidulans* monoculture and the *gcnE* deletion mutant. *p < 0.05

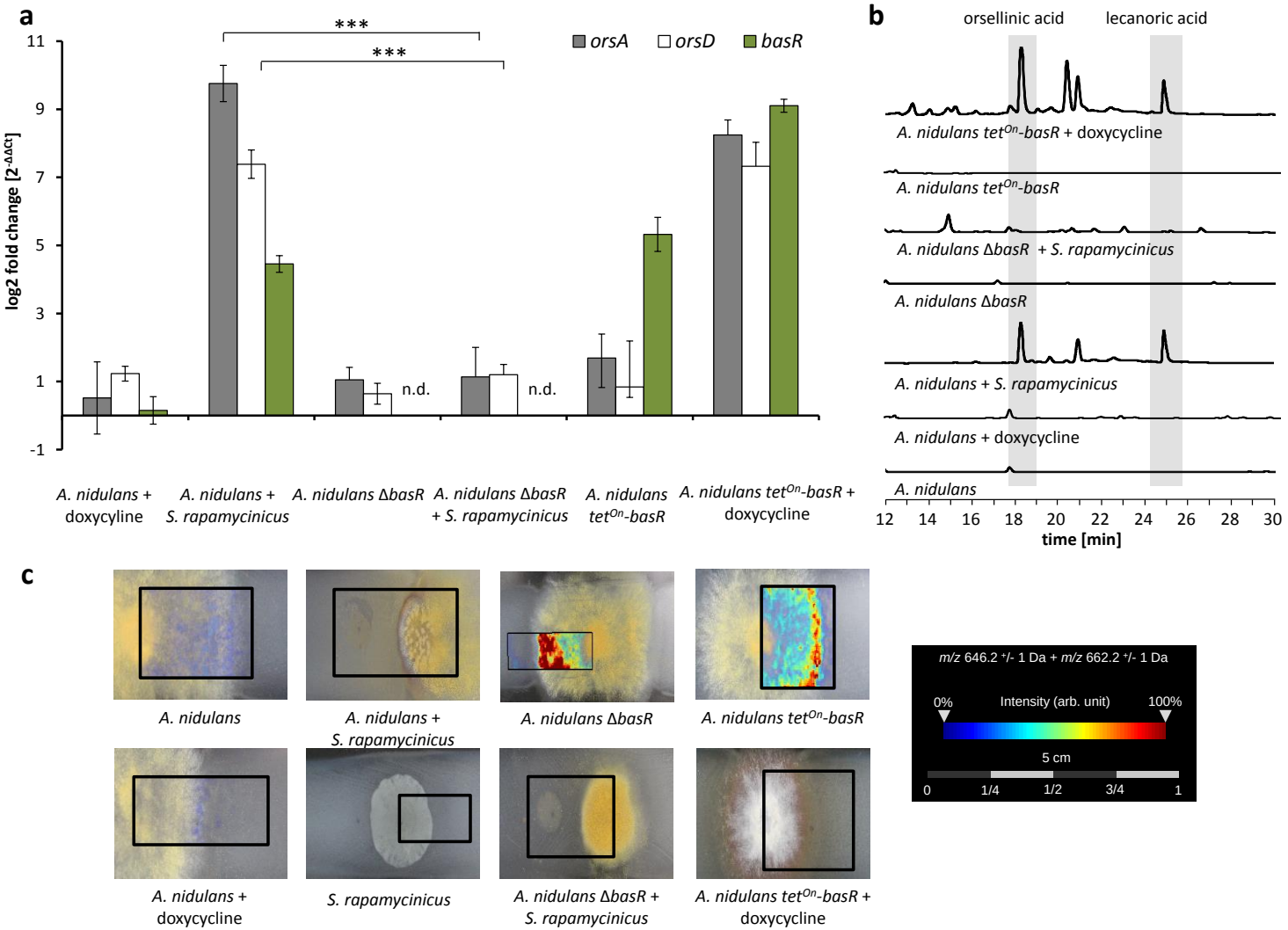

Figure 5. The Myb-like transcription factor BasR of *A. nidulans* is required for *S. rapamycinicus*-triggered regulation of SMs. (**a**) Relative transcript levels of *ors* cluster genes *orsA*, *orsD* and *basR* after 6 hours of cultivation in Δ*basR* mutant strain and *tet*^{On}-*basR* overexpression strain

601 incubated with and without doxycycline. Transcript levels were measured by qRT-PCR normalized to β-actin transcript levels. (**b**) HPLC-based
602 detection of orsellinic and lecanoric acid in wild-type strain, *basR* deletion mutant and *basR* overexpression strain. (**c**) Visualization of ions *m/z*
603 646.3 and *m/z* 662.3 $^{+}$/- 1 Da, potentially corresponding to $[M+Na]^{+}$ and $[M+K]^{+}$ of emericellamide E/F ($C_{32}H_{57}N_5O_7$; accurate mass 623.4258), by
604 MALDI-MS imaging. Images corrected by median normalization and weak denoising. n.d.: not detectable; ***$p < 0.001$

605

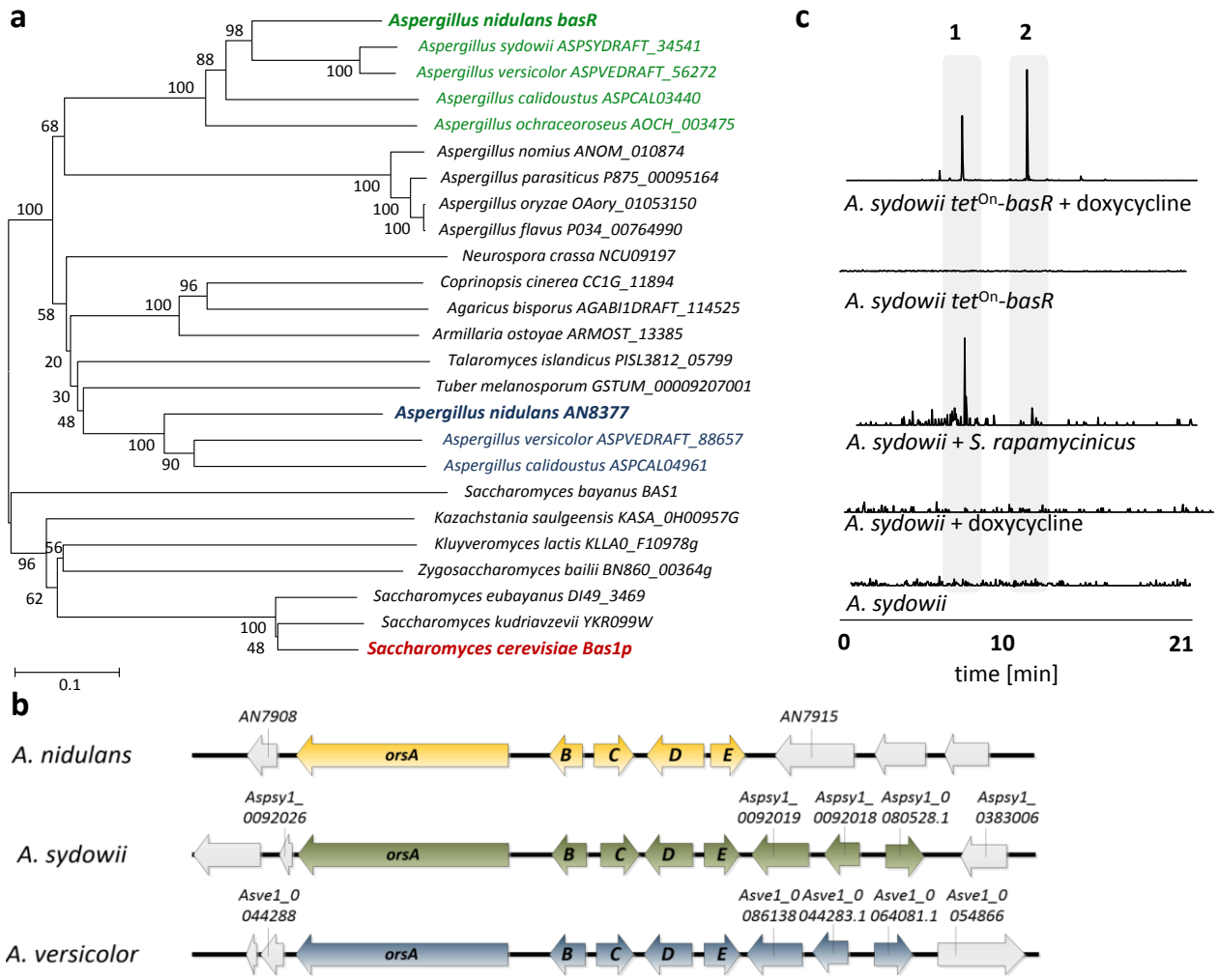

Figure 6. Co-occurrence of BasR and the orsellinic acid gene cluster in other fungi is linked to the *S. rapamycinicus* triggered *ors* gene cluster activation. (a) Phylogenetic analysis of BasR (*AN7174;* green) showing its position among other fungi. The percentage of trees in which the

associated taxa clustered together is shown next to the branches. The names of the selected sequences are given according to their UniProt accession numbers. **(b)** Alignment of the orsellinic acid gene clusters in the fungal species containing a *basR* homologue (*A. nidulans*, *A. sydowii*, *A. versicolor*), where *orsA* encodes the polyketide synthase, while *orsB*-*orsE* code for tailoring enzymes. **(c)** LC-MS-based detection of orsellinic and lecanoric acid in monoculture of the *A. sydowii basR* overexpression strain following induction with doxycycline (left) and during co-cultivation of *A. sydowii* and *S. rapamycinicus* (right). LC-MS profiles of the extracted ion chromatogram (EIC) are shown for *m/z* 167 $[M - H]^-$, which corresponds to orsellinate. Orsellinic (1) and lecanoric acid (2) were detected *via* its fragment ion orsellinate.

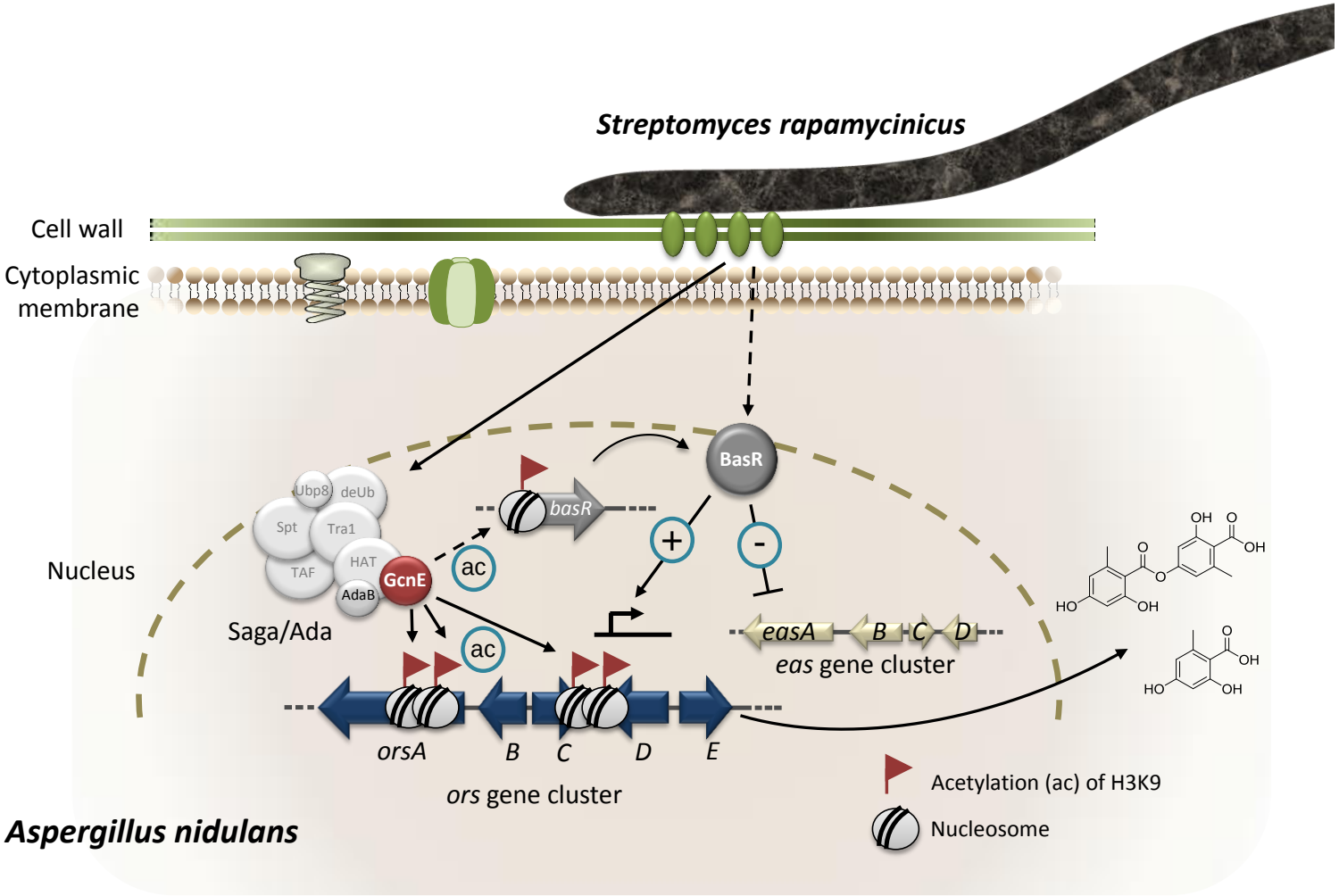

Figure 7. **Model of the *S. rapamycinicus* – *A. nidulans* interaction.** Co-cultivation leads to activation of the *basR* gene. The lysine acetyltransferase GcnE specifically acetylates (ac) lysine (K) 9 of histone H3 at the *ors* gene cluster and presumably at the *basR* gene promoter. As a consequence, *basR* is expressed. The transcription factor BasR activates the *ors* gene cluster and suppresses (-) the expression of the emericellamide (*eas*) gene cluster. The involvement of AdaB and GcnE of the Saga/Ada complex has been experimentally proven (4).

Supplementary Information

SI Material and Methods

ChIP coupled to quantitative RT-PCR (qRT-PCR). Cultures were grown as described in the cultivation part. After 3 hours the isolated DNA was cross-linked to proteins as described before (1). Powdered mycelium was dissolved in 1 mL of sonication buffer (1) and 330 µL aliquots were then subjected to sonication for 30 min with cycles of 2 min maximum intensity followed by a 1 min pause. Sheared chromatin was separated from cell wall debris and incubated with 40 µL of a protein A slurry for 30 min at 4 °C on a rotary shaker. A purified 1:10 dilution of the supernatant was then incubated overnight at 4 °C with 3 µL of antibody directed against the desired target. Antibodies were precipitated with 40 µL of Dynabeads (Invitrogen, Carlsbad, USA) and were immediately incubated with the sample for 40 min at 4 °C on a rotary shaker. Samples were washed 3 times with low salt buffer (1) followed by one time washing with high salt buffer (1). Washed beads were dissolved in 125 µl TES buffer and reverse cross-linked with 2 µL of 0.5 M EDTA, 4 µL of 1 M Tris-HCl pH 6.5 and 2 µL of 1 mg/mL proteinase K for 1 hour at 45 °C. Subsequent DNA purification was conducted with a PCR purification kit and samples were eluted in 100 µL of 1:10 diluted elution buffer. The DNA concentration of genes of interest was quantified using qRT-PCR as described above. Antibodies used are the following: mouse monoclonal ANTIFLAG M2 (Sigma-Aldrich, F3165-5MG, Taufkirchen, Germany), rabbit polyclonal anti-histone H3 (Abcam 1791, Cambridge, UK), rabbit polyclonal histone H3K9ac (Active Motif, Catalog No: 39161, La Hulpe, Belgium) and rabbit polyclonal anti-acetyl-histone H3 (Lys14) (Merck Millipore, Darmstadt, Germany).

24 **ChIP-seq pre-processing.** The *A. nidulans* FGSC A4 genome and annotation (version s10-
25 m03-r28) were obtained from the *Aspergillus* Genome Database (AspGD) (2). The *S.*
26 *rapamycinicus* NRRL 5491 genome was obtained from NCBI (GI 521353217). Both genomes
27 were concatenated to a fused genome which served as the reference genome for
28 subsequent mapping. Raw ChIP-seq reads were obtained by using FastQC v0.11.4. Trimming
29 and filtering were achieved by applying Trim Galore utilizing Illumina universal adapter and
30 phred+33 encoding. Reads were not de-duplicated since the duplication rate was < 15% for
31 most libraries. Bowtie2 (version 2.2.4) using default parameters was employed to map reads
32 to the fused genome. Quantification of reads was carried out using the Bioconductor
33 'GenomicAlignments' package forming the basis for three subsequent approaches. Firstly, a
34 genome-wide equi-spaced binning across the genome with different resolutions (50k and 2k
35 bp bins) counting reads overlapping each bin was applied. Library normalization on bin
36 counts was performed by only considering reads mapping to the *A. nidulans* genome.
37 Secondly, reads overlapping genes were counted, using the AspGD (2) annotation. They
38 formed the basis for the subsequent DCS analysis (see below). Thirdly, average profile plots
39 to assess relative histone distributions around TSS and TTS were generated using the
40 bioconductor package regioneR(3).
41 **DCS analysis.** To identify genes exhibiting differences in their chromatin state, we employed
42 the bioconductor package edgeR (4) originally developed for RNA-seq differential expression
43 analysis. The ChIP-seq data follow the same pattern, *i.e.*, negative binomial distribution of
44 reads. Library normalization was achieved with the trimmed mean of M values (4) method
45 only based on *A. nidulans* gene counts for calculating the effective library sizes, not taking
46 into account reads mapping to *S. rapamycinicus* which would otherwise artificially influence

47 the effective library size. Comparisons were made between libraries for all ChIP targets
48 separately obtained from monocultures of *A. nidulans* and co-cultures with *S. rapamycinicus.*
49 These targets were H3, H3K9ac and H3K14ac. Results including normalized read counts
50 (RPKM) statistics and LFCs are reported in Table S2. Normalized counts and LFCs were also
51 further used for comparisons with the corresponding microarray-based gene expression and
52 the calculated LFCs.

53 **MACS analysis.** Candidate peaks were identified using two methods: a differential binding
54 analysis (EdgeR) and a peak-calling approach (MACS, version 2.0.1) (5). The peak caller
55 performed several pairwise comparisons between samples with the same antibody and
56 different conditions in order to retrieve the peaks with significant change of ChIP signal
57 indicating differential binding for that particular comparison. The program kept the track of
58 different replicates, the signal was reported per million reads and produced a BED format
59 track of the enriched regions, other parameters were used with default values. The BED files
60 were subsequently converted to Big Wig format for visualization through the tool Integrative
61 Genomics Viewer(6).

62 **Extraction of fungal compounds, HPLC and LC-MS analyses.** Culture broth containing fungal
63 mycelium with and without bacteria was homogenized utilizing an ULTRA-TURRAX (IKA-
64 Werke, Staufen, Germany). Homogenized cultures were extracted twice with 100 mL ethyl
65 acetate, dried with sodium sulfate and concentrated under reduced pressure. For HPLC
66 analysis, the dried extracts were dissolved in 1-1.5 mL of methanol. Analytical HPLC was
67 performed using a Shimadzu LC-10Avp series HPLC system composed of an autosampler,
68 high pressure pumps, column oven and PDA. HPLC conditions: C18 column (Eurospher 100-5
69 250 x 4.6 mm) and gradient elution (MeCN/0.1 % (v/v) TFA (H_2O) 0.5/99.5 in 30 min to

70 MeCN/0.1 % (v/v) TFA 100/0, MeCN 100 % (v/v) for 10 min), flow rate 1 mL min^{-1}; injection
71 volume: 50 µL.
72 The samples of *A. sydowii* were loaded onto an ultrahigh-performance liquid
73 chromatography (LC)–MS system consisting of an UltiMate 3000 binary rapid-separation
74 liquid chromatograph with photodiode array detector (Thermo Fisher Scientific, Dreieich,
75 Germany) and an LTQ XL linear ion trap mass spectrometer (Thermo Fisher Scientific,
76 Dreieich, Germany) equipped with an electrospray ion source. The extracts (injection
77 volume, 10 µL) were analyzed on a 150- by 4.6-mm Accucore reversed-phase (RP)-MS
78 column with a particle size of 2.6 µm (Thermo Fisher Scientific, Dreieich, Germany) at a flow
79 rate of 1 mL/min, with the following gradient over 21 minutes: initial 0.1% (v/v) HCOOH-
80 MeCN/0.1% (v/v) HCOOH-H_2O 0/100, which was increased to 80/20 in 15 min and then to
81 100/0 in 2 min, held at 100/0 for 2 min, and reversed to 0/100 in 2 minutes.
82 Identification of metabolites was achieved by comparison with an authentic reference.
83 Samples were quantified *via* integration of the peak area using Shimadzu Class-VP software
84 (version 6.14 SP1).
85 **Generation of *A. nidulans* deletion strains.** The transformation cassettes for the *basR* and
86 *AN8377* deletion strains were constructed as previously described (7). Approximately ~1000-
87 bp sequences homologous to the regions upstream and downstream of *basR* and *AN8377*
88 were amplified and fused to the *argB* deletion cassette (8). Transformation of *A. nidulans*
89 was carried out as described before (9).

90 **Generation of inducible *A. nidulans* and *A. sydowii basR* overexpressing mutant strains.**
91 For overexpression of *basR*, the tetracycline-controlled transcriptional activation system
92 (tet^{On}) was used (10). The *basR* gene sequences together with their ~1000-bp flanking

93 regions were amplified from *A. nidulans* and *A. sydowii* genomic DNA. The *tet*^{On}-system was
94 amplified from plasmid pSK562. All DNA fragments were assembled by using NEBuilder HiFi
95 DNA Assembly Master Mix (New England Biolabs, Frankfurt, Germany). The *A. nidulans*
96 *pabaA*1 gene was used as a selectable marker to complement the *p*-aminobenzoic acid
97 auxotrophy of the *A. nidulans* Δ*basR* mutant. For *A. sydowii*, the *Aspergillus oryzae hph*
98 cassette was used as the selectable marker. 200 µg/mL hygromycin (Invivogen, Toulouse,
99 France) were used for selection of transformant strains.

100 **Measurement of amino acids.** Amino acids were extracted from 10 mg samples with 1 mL of
101 methanol and the resulting extract was diluted in a ratio of 1:10 (v:v) in water containing the
102 ^{13}C, ^{15}N labeled amino acid mix (Isotec, Miamisburg, Ohio, USA). Amino acids in the diluted
103 extracts were directly analyzed by LC-MS/MS as described with the modification that an
104 API5000 mass spectrometer (Applied Biosystems, Foster City, California, USA) was used (11).

105

106 ## SI Results

107 **Details of the ChIP analysis**

108 After first examination, we found that a significant proportion of co-incubated library reads
109 originated from *S. rapamycinicus*. A fused genome concatenating the *A. nidulans* and the *S.*
110 *rapamycinicus* genomes was generated. About 90-98% of the reads mapped against the
111 fused genome (Table S2), which suggested a high quality of sequencing data. This
112 assumption was confirmed by examining the quality of libraries using FastQC (data not
113 shown). As indicated, the coverage was substantially higher on the *S. rapamycinicus* genome
114 with only ~20 % mapping to the *A. nidulans* genome (see Table S2). Expectedly, this ratio has
115 shifted considerably towards the *A. nidulans* genome for histone targeting ChIP libraries (Fig.

116 1 a) going up from 20 % to around 90 % for all H3, H3K9 and H314 libraries validating correct
117 antibody enrichment as *S. rapamycinicus* is devoid of histones. However around 10 % of
118 reads were still mapping to the *S. rapamycinicus* genome which might be due to imperfect
119 antibody specificity. Coverage depth deviations were accounted for by only considering
120 reads originating from *A. nidulans*. This allowed for calculation of library size factors used for
121 library normalization. To assess antibody specificity, we calculated the fraction of reads
122 mapping to mitochondria, which do not contain histones. The control library amounted to
123 about 0.25 % of reads as opposed to about 0.01-0.03 % for H3, H3K9ac, H3K14ac libraries
124 constituting a 10-fold enrichment. As a background control we used ChIP material obtained
125 from anti-FLAG-tag antibody precipitates of a non-tagged fungal wild-type strain co-
126 cultivated under the same conditions with *S. rapamycinicus.*
127 We quantified the relative library proportions which amounted to 8-17 % of H3, H3K14ac
128 and H3K9ac as well as up to ~65 % for background reads of co-incubated libraries mapped to
129 *S. rapamycinicus* (Table S2). However, the background read proportions might not
130 necessarily reflect actual gDNA ratios of both species in the co-cultivation due to various
131 potential biases. To examine read distribution for each library, we counted mapped reads
132 within equally spaced bins along the fused genome for different resolutions (see methods
133 and Fig. 1 a & b). As expected, background reads (upper panel of Fig. 1 a) were evenly
134 distributed across the genome reflecting nonspecific targeting of particular areas. The fused
135 genome further enabled for controlling correct co-incubation conditions since no reads
136 should be mapping to *S. rapamycinicus* in non-co-incubated samples as can be seen in Fig.
137 1 a in the right panels (blue lines). The co-incubated samples exhibit an increased coverage
138 in the middle of the *S. rapamycinicus* genome which might be due to sequence biases or

139 enriched DNA caused by the replication origin (*oriC*) located in this region (12). Further,
140 there were coverage dips in the middle of the fungal chromosomes (see Fig. 1 a), which were
141 most likely due to incomplete assembly around the centromeres which are characterized by
142 long 'N' stretches (13).

143 **Changes of H3K9 and H3K14 acetylation profiles in *A. nidulans* in response to *S.***
144 ***rapamycinicus***

145 As reported in the manuscript, the genome-wide H3K9 and H3K14 chromatin landscape of *A.*
146 *nidulans* was determined. There was also a drop-off in all libraries at the chromosome arms,
147 which was most likely caused by the bordering bins being shorter and therefore account for
148 less reads. Since gene density also varies across the genome (lower panel of Fig. 1 a), we
149 addressed the question whether this correlates with the intensity of the investigated
150 chromatin states. To this end, we calculated the spearman correlation to correlate the read
151 counts and the gene counts among the 50k bins. As expected, there was almost no
152 correlation between the background and the genes (r = 0.09). However, for H3 we found it
153 to be rather high (r = 0.37) (Fig. S4). Since the used bin size is large, this could point at global
154 H3 occupancy to be higher for high gene density regions such as euchromatin and low H3
155 occupancy for heterochromatin. Noteworthy, the correlation between read and gene
156 density was found to be lower for H3K14ac and H3K9ac (r=0.14 and 0.15 respectively), which
157 might indicate a more subtle regulatory mechanism for those marks targeting individual
158 genes as opposed to larger domains. Notably, the highest correlation was found between
159 the two acetylation marks (r=0.53) hinting at some potential cross-talk or common
160 regulation between them (Fig. S5).

161

162

163 **Chromatin profiles at translation start sites and translation termination sites**

164 We assessed the location of H3K9ac, H3K14ac and histone H3 relative to promoters and
165 gene bodies by plotting the average read count frequency for all genes to either the TSS or
166 TTS (Fig. S1) (14). Due to missing information about the 5' and 3' transcriptional start and
167 stop sites, we used translational start and stop sites for transcription start and stop sites,
168 respectively, as surrogates. The results obtained apply to both *A. nidulans* in mono- and co-
169 culture with the bacterium. According to Kaplan et al. (15), the peaks correspond to highly
170 positioned nucleosomes relative to the TSS with a nucleosome-free region (NFR) directly
171 upstream of the TSS. H3K9ac and H3K14ac showed highest enrichment for the first and
172 second nucleosomes up- and downstream of the TSS and drastic reduction downstream of
173 the third nucleosome after the TSS (Fig. S1). Reduced occupancy of unmodified histone H3
174 was observed at the TSS(15). Towards the 3' end of genes, histone H3 occupancy gradually
175 increased, which was accompanied by a decrease in acetylation. Plotting of differentially
176 acetylated H3K9ac against H3K14ac showed a strong correlation between the localization of
177 the two modifications (Fig. S14 a). Acetylation is generally described as an transcription
178 activating mark(16). To test for this general assumption we correlated our acetylation data
179 to microarray data generated under the same condition(17) (Fig. S14 b). This allowed us to
180 compare the log-fold changes (LFCs) of the differential chromatin states with the LFCs
181 calculated from the RNA expression data. H3K9ac correlates to the differentially expressed
182 genes with a coefficient of 0.5 in contrast to H3K14ac (-0.05) and histone H3 (-0.01) for
183 which no detectable dependency was determined (Fig. S3). Similarly, Fig. S3 shows the same
184 trend, i.e., a correlation of 0.2 for gene expression changes *versus* H3K9ac changes which is

185 expected since the calculation included all genes of which most did not change. To
186 determine the correlation of acetylation at the TSS and the TTS according to the grade of
187 expression of the genes, we separated the differentially expressed genes into four quartiles
188 (q1 lower 25 %, q2 the medium lower 25 – 50 %, q3 are the medium higher 50-75 %, q4
189 higher 25 %). The increase of acetylation at the TSS correlated with the expression level of
190 genes (Fig. S12 a & c). Decreased expression coincided with an increase of histone H3 at the
191 TSS (Fig. S12 e).

192 **Reduced intracellular amino acid concentration in response to the bacterium**

193 The increased expression of *cpcA* and other genes involved in amino acid biosynthesis
194 implied a reduced availability of amino acids in the cell upon bacterial-fungal co-cultivation.
195 Therefore, we measured the internal amino acid pool in *A. nidulans* both grown in
196 monoculture and with *S. rapamycinicus* (Fig. S13). As an additional control and to further
197 confirm the specificity of the interaction, the fungus was co-cultivated with *Streptomyces*
198 *lividans*, which does not induce the *ors* gene cluster. As shown in Fig. S13, significantly
199 reduced levels of glutamine, histidine, phenylalanine, asparagine, threonine and reduced
200 metabolism of arginine, which was supplemented to the medium, were observed. The
201 monoculture of *A. nidulans,* co-cultivation of *A. nidulans* with *S. lividans* as well as the
202 addition of *S. rapamycinicus* after 24 hours of fungal cultivation served as controls. All of the
203 controls showed comparable amino acid levels.

204

205

206

207

208 **Supplementary figures**

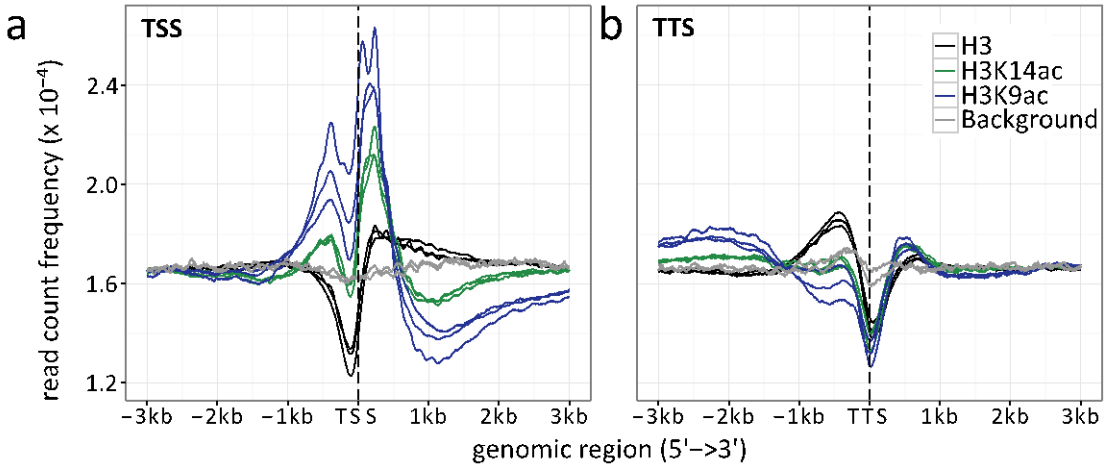

209

210 **Figure S1. Read count frequencies for (a) TSS and (b) TTS.** Lines correspond to the relative
211 enrichment of ChIP signal strength relative to the TSS/TTS averaged across all genes. ChIP-
212 seq read count serves as a surrogate for signal strength (see methods for further details).
213 Compared were the enrichment of histone H3 (black), H3K9ac (blue), H3K14ac (green) and
214 the background control (grey) over an average of all TSS and TTS. The enrichment curves for
215 all biological replicates are given, indicated by multiple lines per enrichment target.

216

217

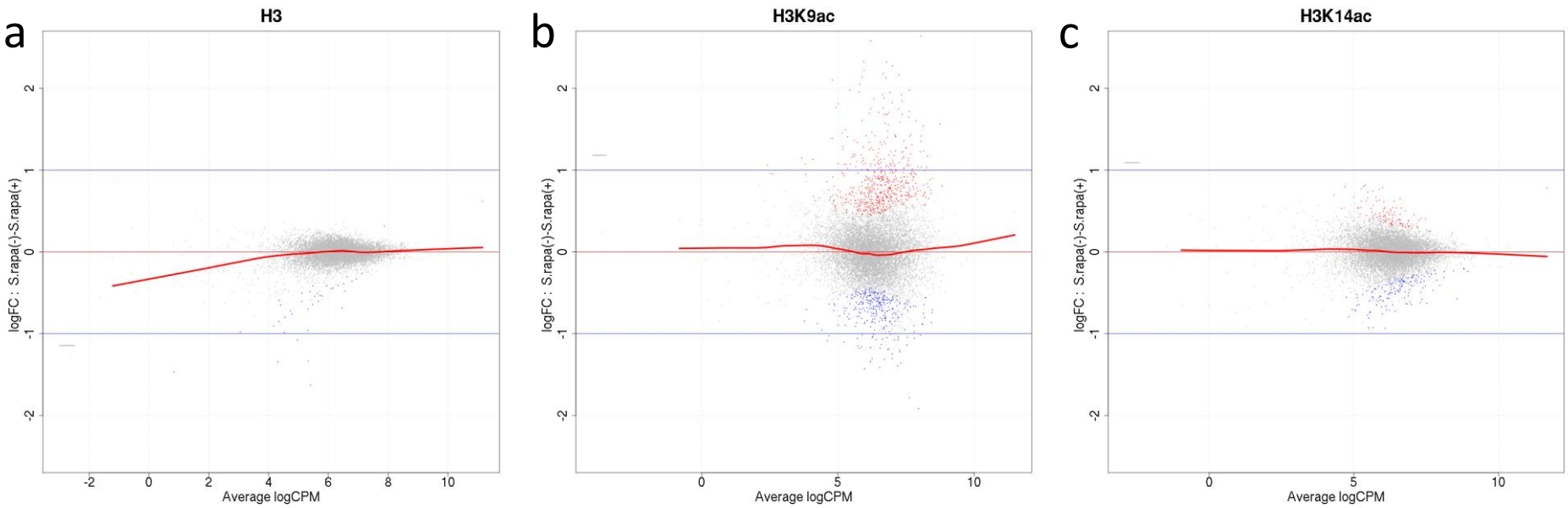

Figure S2. Mean average (MA) plots comparing normalized ChIP-seq LFCs H3(Cterm) (a), H3K14ac (b) and H3K9ac (c) of each gene between *A. nidulans* monoculture and co-culture for antibodies used in this study. Y-axis indicates LFCs of ChIP signal between mono- and co-culture for each gene which corresponds to the dots. X-axis indicates mean intensity of ChIP signal of both conditions. Genes were colored according to DCS outcome with grey indicating genes with no significant change of ChIP signal, red and blue indicate genes showing respective higher or lower signal in co-culture.

ChIP-seq/ Microarray log_2 fold change for all genes:
A. nidulans vs. *A. nidulans* + *S. rapamycinicus*

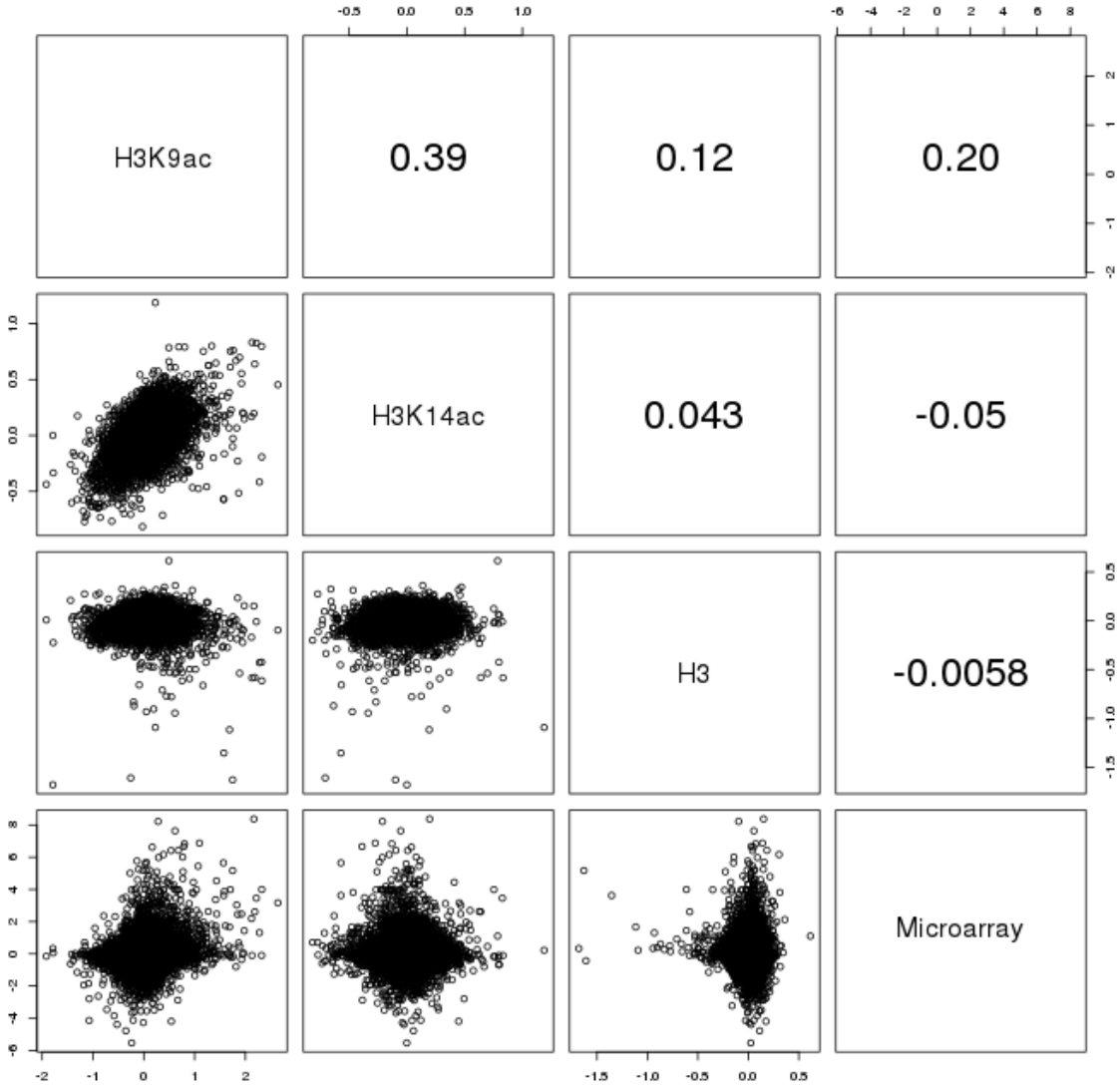

Figure S3. Correlation of data points for LFCs of ChIP-seq with LFCs of microarray data for all *A. nidulans* genes, depicting single data points and the correlation coefficient.

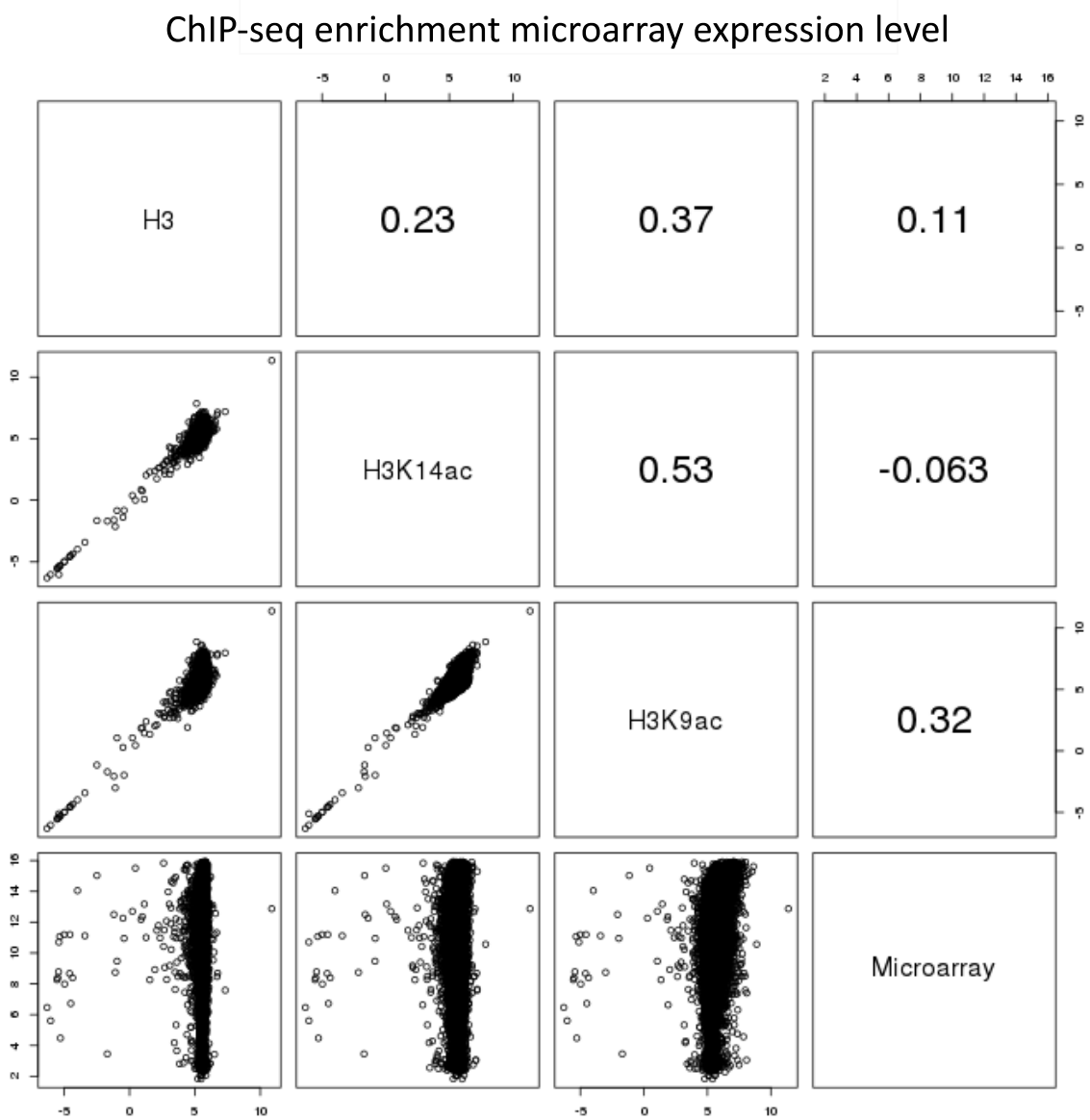

234

235 **Figure S4. Pairwise comparison of ChIP-seq and microarray intensities of all genes in *A.***
236 ***nidulans* monoculture.** The numbers resemble the correlation coefficient for the respective
237 comparison. Intensity defines enrichment of number of reads per gene.

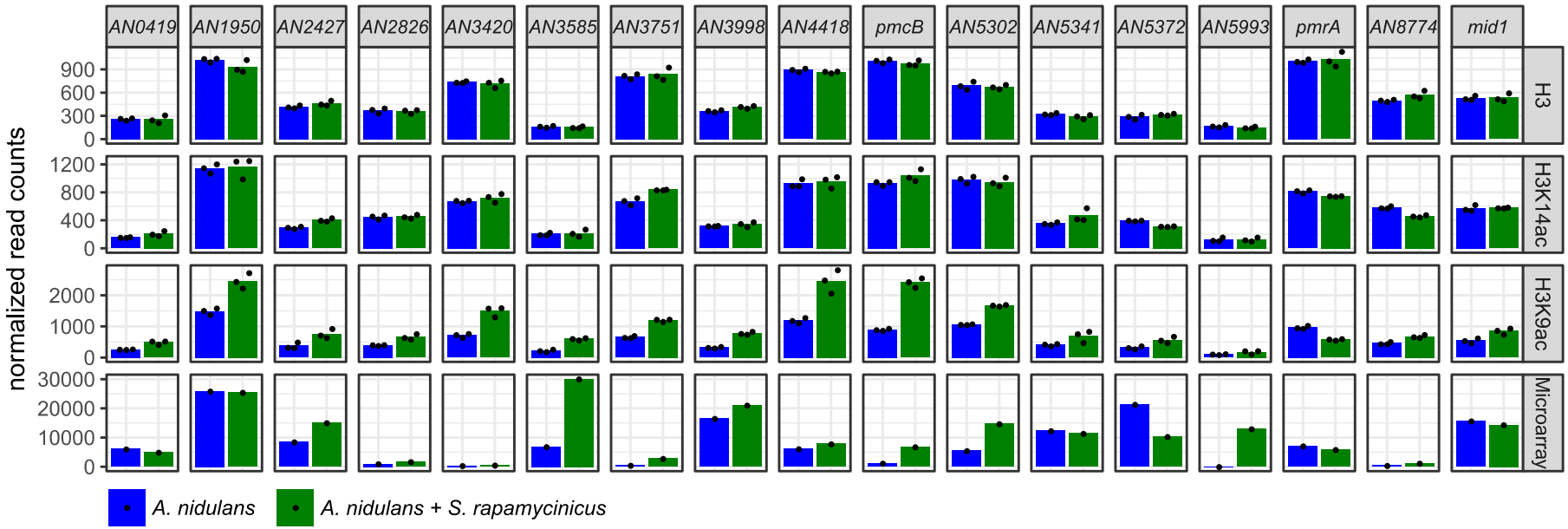

Figure S5. Normalized ChIP-seq read counts were used to quantify the chromatin state for individual genes. Here, for H3, H3K14ac and H3K9ac libraries genes involved in calcium signaling are shown. Counts were obtained by counting reads mapping to the promoter area for each gene that is 500 bp down- and 1000 bp upstream from the TSS. Depicted bars are calculated from three data points.

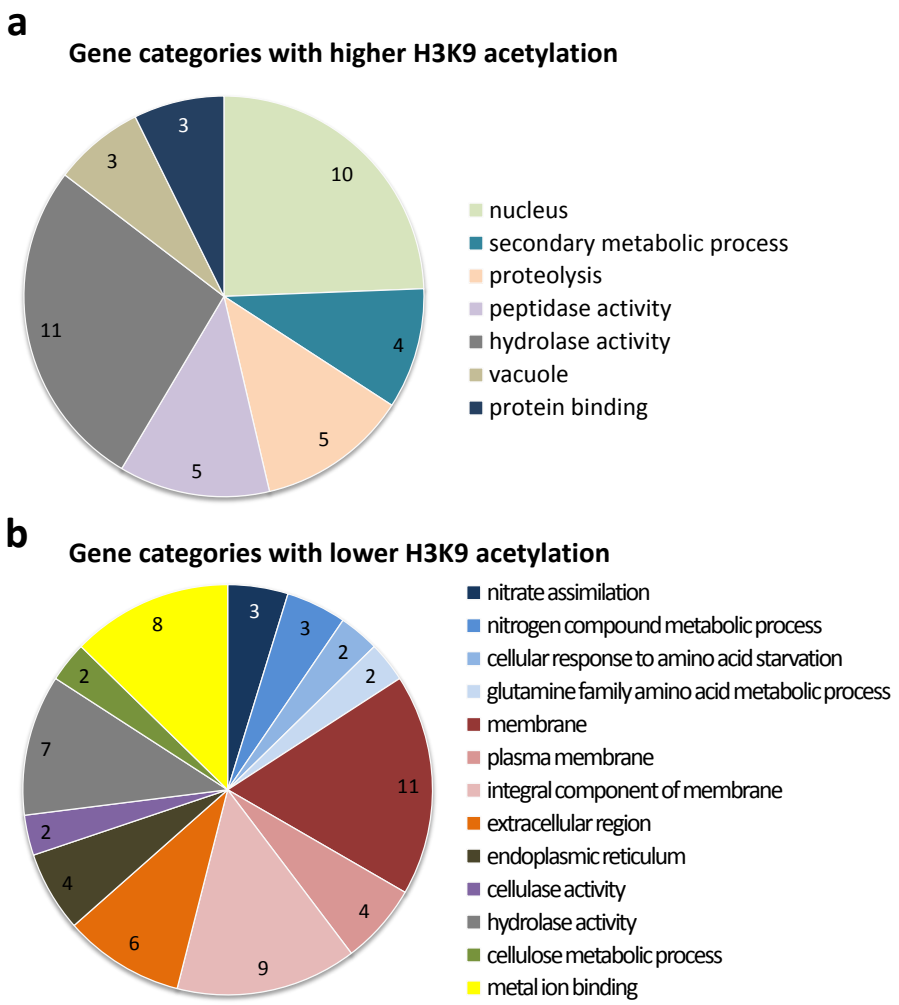

Figure S6. Gene ontology of the 15 most significantly enriched categories for differentially higher and lower acetylated genes at H3K9 upon co-cultivation with *S. rapamycinicus*. Functional categorization of differentially higher (A) and lower (B) acetylated genes, possessing a *p* value < 0.05, with FungiFun2 (18). Overrepresented categories having a p value < 0.01.

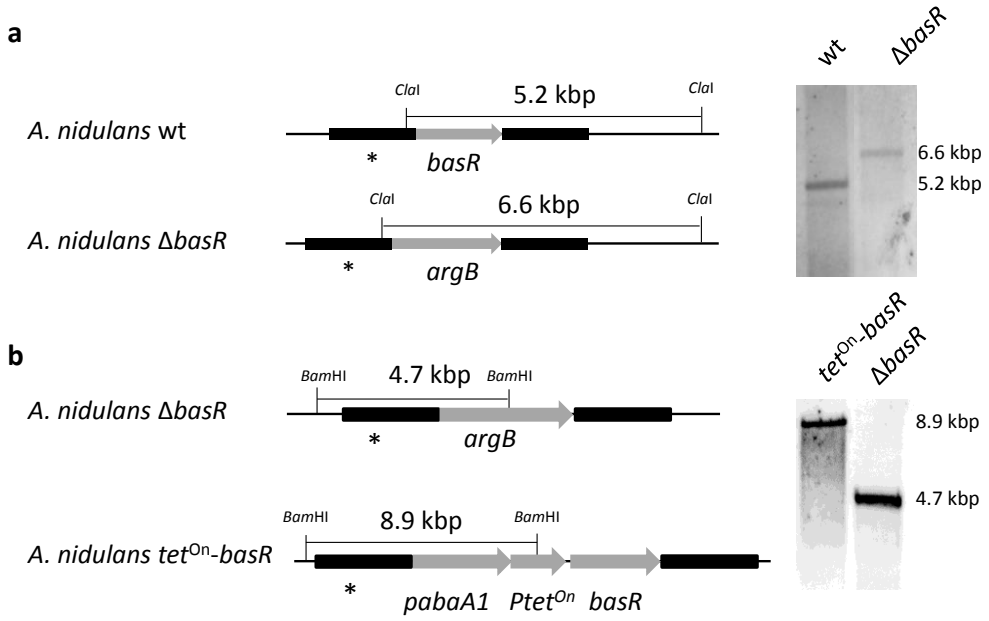

Figure S7. Generation of a *basR* deletion mutant and inducible overexpression strain based on the *A. nidulans* wild-type strain A1153. (**a**) Genomic organization of *basR* and Southern blot analysis of *basR* deletion. The *basR* gene was replaced by the *argB* gene. Transformant strains were checked with a probe (*) directed against the flanking region of the construct. Genomic DNA was digested with *Cla*I. wt, wild-type strain as a control. (**b**) Generation of the inducible *basR* overexpression strain by complementation of the *basR* deletion strain. The *tet*^{On}-*basR* gene cassette was integrated at the Δ*basR* genomic locus using the *pabA1* gene as selectable marker replacing the *argB* marker. Genomic DNA was cut with *Bam*HI. Transformant strains were checked with a probe (*) directed against the flanking region of the construct.

Figure S8. Molecular phylogenetic analysis of BasR (*AN7174*). The tree reports distances between BasR-similar amino acid sequences identified by BlastP analysis using the entire sequences. The percentage of trees in which the associated taxa clustered together is shown

270 next to the branches. The BasR proteins from *A. nidulans*, *A. calidoustus*, *A. sydowii*, *A.*
271 *versicolor*, *A. rambellii* and *A. ochraceoroseus* form a separate clade (reported in green),
272 while the yeast Bas1p-related sequences are more distantly related to BasR (in red). The
273 second similar Myb-like transcription factor from *A. nidulans* (*AN8377*) forms a clade with
274 orthologues from *A. calidoustus* and *A. versicolor* (in blue), which seems to be more related
275 to Bas1p than to BasR. The names of the selected sequences are given according to their
276 UniProt accession numbers.

277

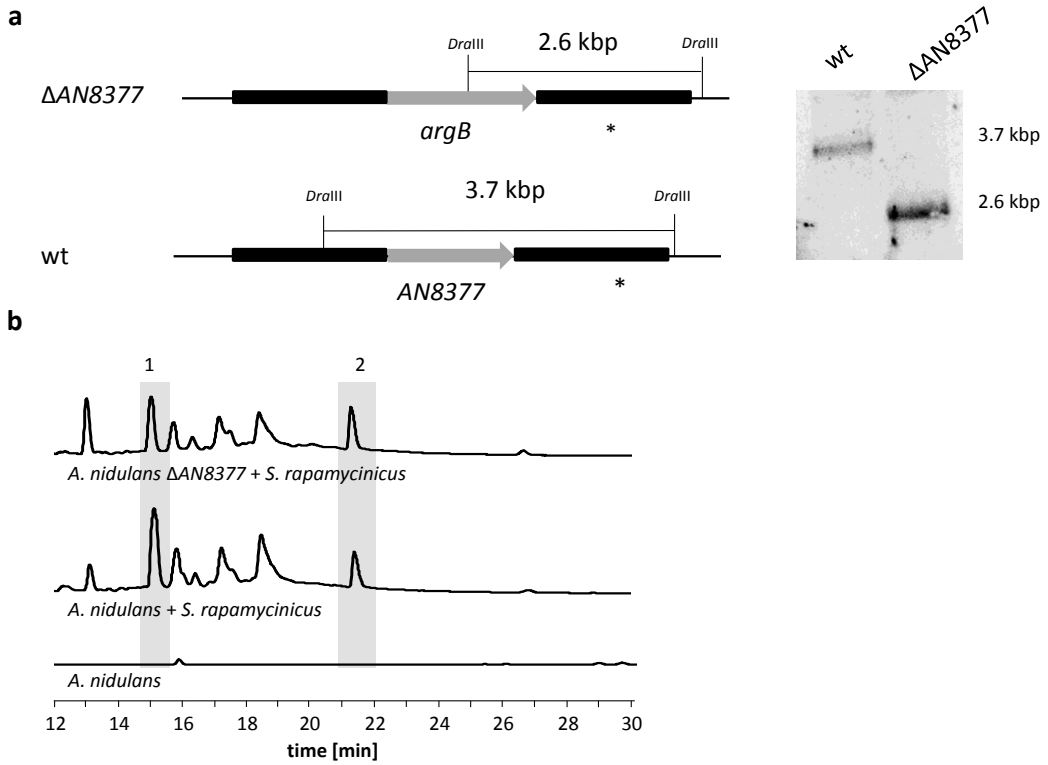

278

279 **Figure S9. Deletion of the second putative *bas1p* homologous gene (*AN8377*) in *A. nidulans***
280 **and analysis of its impact on the *ors* gene cluster induction in response to *S.***
281 ***rapamycinicus.*** (**a**) Chromosomal organization of the *A. nidulans AN8377* gene before and
282 after deletion. The gene *AN8377* was replaced by an *argB* cassette in *A. nidulans* wild-type
283 strain A1153. Genomic DNA was digested with *Dra*III. A PCR fragment covering the
284 downstream sequence of *AN8377* was used as a probe (*). wt, wild-type strain as a control.
285 (**b**) LC-MS-based detection of orsellinic acid (1) and lecanoric acid (2) in the co-cultivation of
286 the *AN8377* deletion mutant with *S. rapamycinicus*.

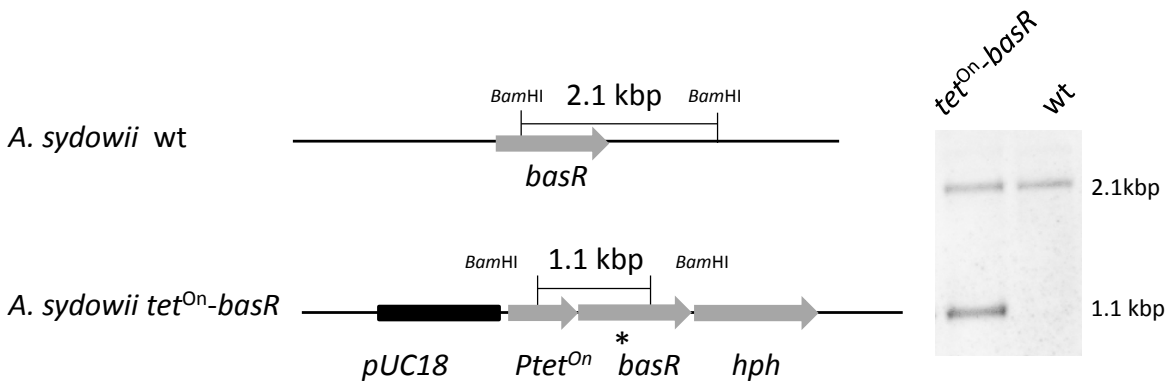

Figure S10. Generation of the inducible *basR* overexpression strain by ectopic integration of an additional copy of the *basR* gene in the *A. sydowii* wild-type strain (wt). The *tet*^{On}-*basR* construct was integrated ectopically into the wild-type genome, using the *hph* cassette as selectable marker. For Southern blot analysis, transformant strains were checked with a probe (*) directed against a region flanking the *tet*^{On} cassette and *basR* gene. The genomic DNA was digested with *Bam*HI.

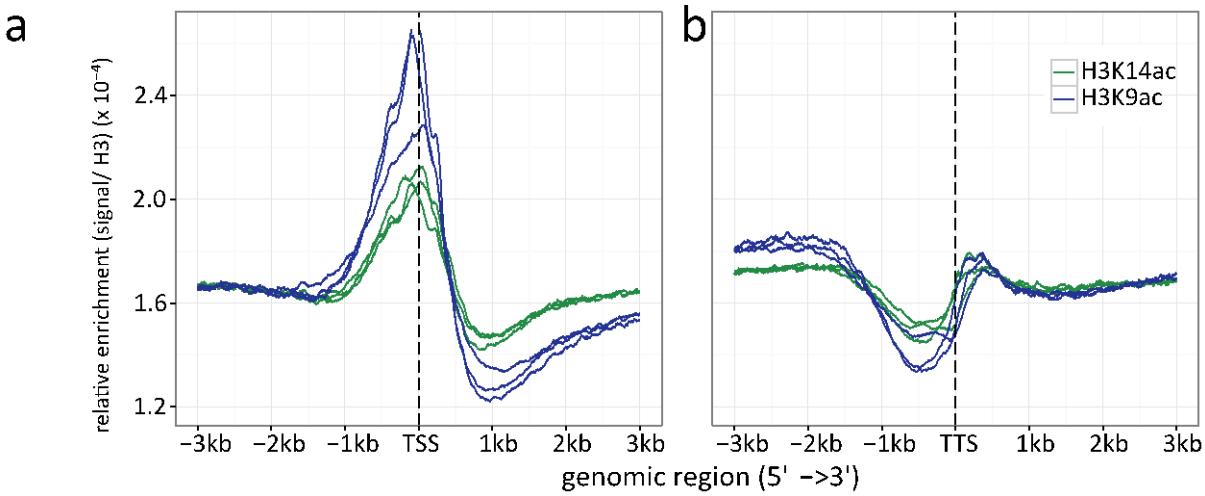

Figure S11. Histone H3 normalized read count frequencies for H3K9ac (green) and K14 ac (blue) at the (a) TSS and (b) TTS. The enrichment is given in signal to H3 ratio. Multiple lines per ChIP target resemble the three independent biological replicates.

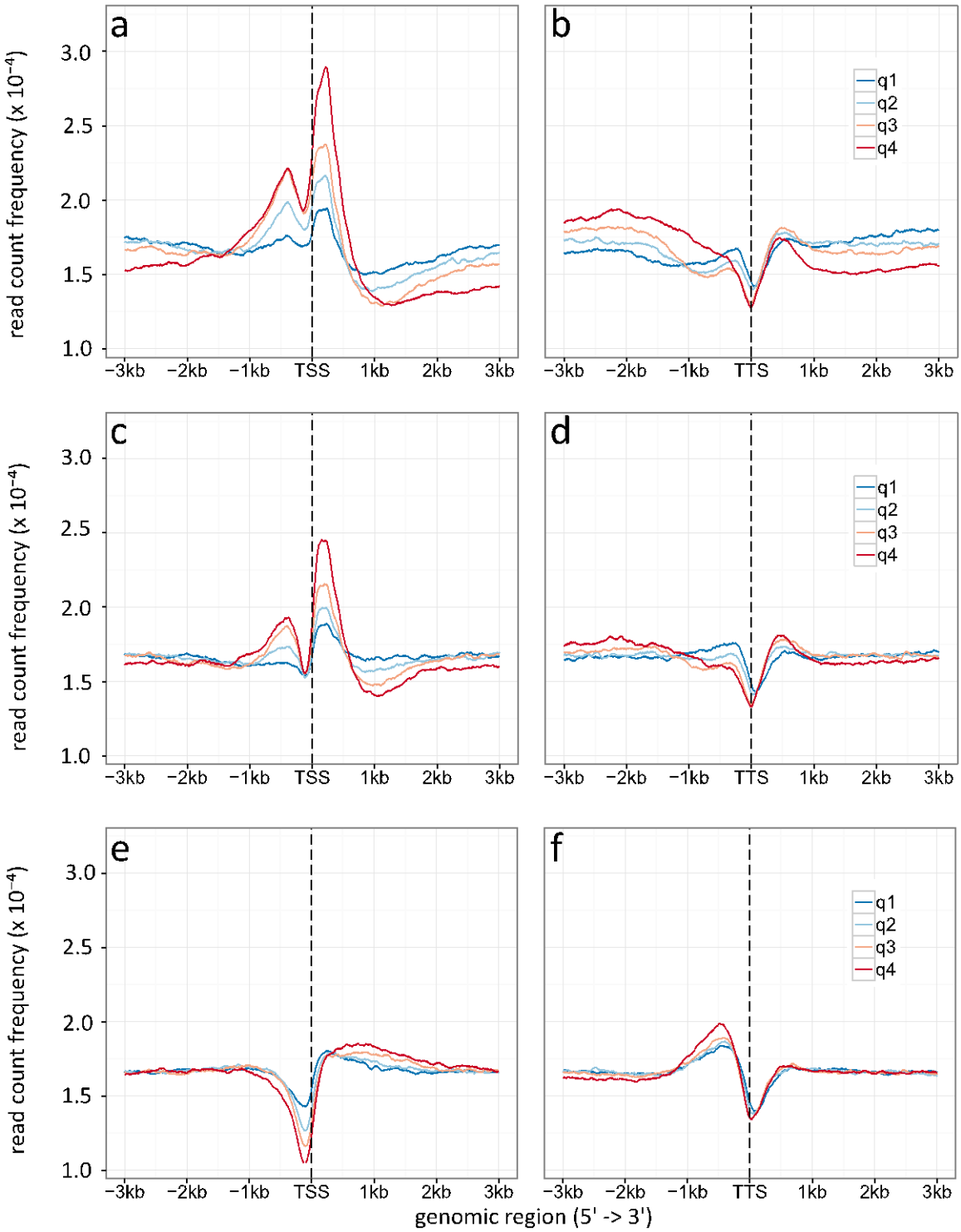

Figure S12. Density plot of TSS (a, c, e) and TTS (b, d, f) given for different gene expression levels (q1-q4). (**a**, **b**) Specific enrichment of H3K9ac, (**c**, **d**) H3K14ac and (**e**, **f**) H3 is given in read count frequency. Thereby q1 are the lower 25 %, q2 the medium lower 25 – 50 %, q3 are the medium high 50-75 %, q4 the higher 25 %.

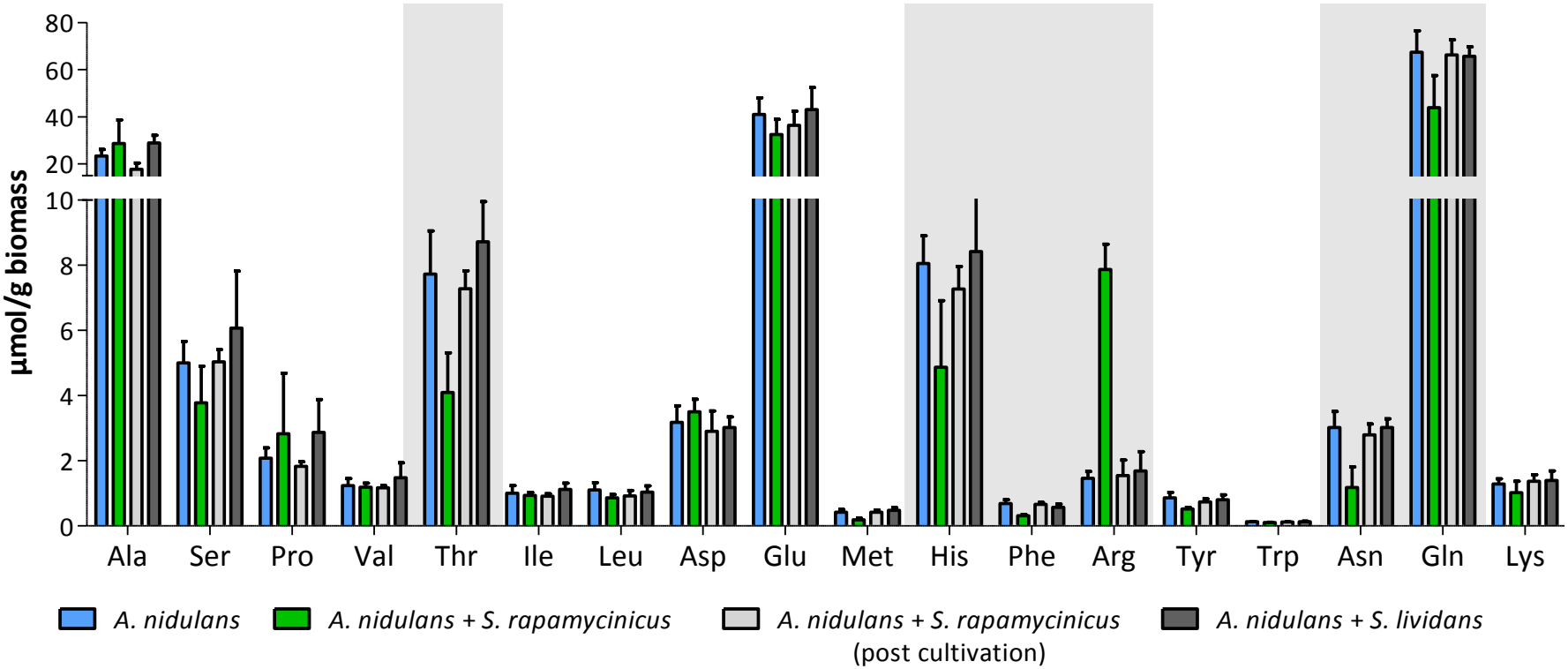

Figure S13. Intracellular amino acid concentration of *A. nidulans* in monoculture and co-culture with *S. rapamycinicus*. Co-cultivation with *S. lividans* and addition of *S. rapamycinicus* after 24 hours of cultivation served as negative controls. Furthermore, before extraction of amino acids the fungus (post cultivation) was also supplemented with *S. rapamycinicus* to exclude a bias resulting from bacterial amino acids. Threonine, histidine, phenylalanine, arginine, asparagine and glutamine showing different concentrations in co-culture compared to monoculture are highlighted in grey.

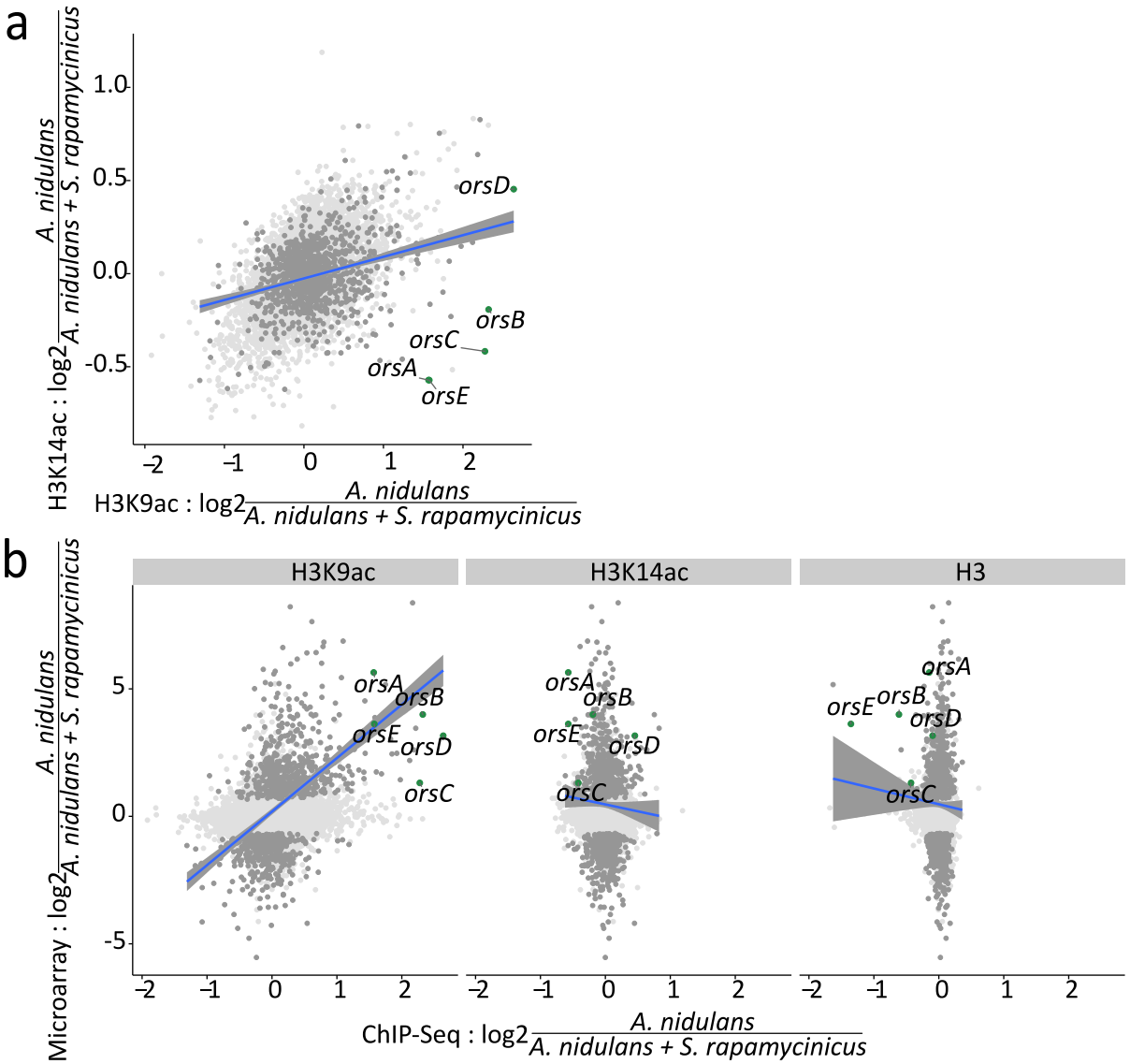

Figure S14. Relation between ChIP-seq and microarray data. The blue lines resemble the linear regression line based on the differentially expressed genes with an adjusted *p*-value of < 0.1 including the confidence interval shown in grey. (**a**) LFCs of H3K14ac plotted against LFCs of H3K9ac. Dots depicted in dark grey and green mark differentially expressed genes and *ors* cluster genes, respectively. (**b**) Pairwise comparison of LFCs of H3, H3K14ac and H3K9ac data with microarray data obtained during co-cultivation of *A. nidulans* with *S. rapamycinicus*.

326 ## Supplementary tables

327 **Table S2.** List of selected genes with differentially acetylated H3K9 and different expression.

			ChIP-seq	Microarray
Name	**Annotation**	**Description**	**LFC H3K9ac**	**LFC**
I - Nitrogen metabolism				
crnA	AN1008	Nitrate transporter with 12 predicted *trans*-membrane domains	-1.30	-0.01
niaD	AN1006	Nitrate reductase (NADPH)	-1.78	-0.04
niiA	AN1007	Nitrite reductase	-1.92	-0.14
tamA	AN2944	Transcriptional co-activator of the major nitrogen regulatory protein AreA	-0.80	-0.35
gltA	AN5134	Glutamate synthase, NAD^+-dependent (GOGAT)	-0.86	-0.46
gdhA	AN4376	NADP-linked glutamate dehydrogenase	-1.14	0.06
ntpA	AN5696	Nitric oxide-induced nitrosothionein involved in NO detoxification	-1.16	-0.21
meaA	AN7463	Major ammonium transporter	-1.22	-0.17
ureD	AN0232	Nickel-binding protein involved in utilization of urea as a nitrogen source	-1.44	-0.95
prnD	AN1731	Proline dehydrogenase with a predicted role in proline metabolism	-1.36	0.02
prnB	AN1732	Proline transporter	-1.39	-0.48
II - Amino acid metabolism				
ugeA	AN4727	UDP-glucose 4-epimerase, involved in galactose metabolism	-0.82	-0.62
qutB	AN1137	Quinate 5-dehydrogenase	-0.90	0.47
	AN9506	Protein with predicted amino acid *trans*-membrane transporter activity	-0.98	-0.68
	AN1923	Putative alanine transaminase	-1.02	0.18
	AN5731	Putative chorismate synthase	-1.04	0.03
	AN6255	Putative cytochrome c oxidase subunit with a predicted role in energy metabolism	-1.08	0.35
	AN8118	Putative cytochrome c oxidase	-1.08	0.33

		subunit with a predicted role in energy metabolism		
	AN1150	Putative transaminase with a predicted role in arginine metabolism	-0.62	0.10
	AN1733	Putative delta-1-pyrroline-5-carboxylate dehydrogenase with a predicted role in glutamate and glutamine metabolism	-0.79	-0.43
	AN2129	Subunit 5 of the COP9 signalosome (CSN) responsible for cleaving the ubiquitin-like protein Nedd8 from cullin-RING E3 ubiquitin ligases	-0.50	-1.16
	AN3347	Putative amino acid transporter	-0.64	Not detectable
	AN8647	High-affinity nitrite transporter	-0.59	-1.96
	AN0399	High-affinity nitrate transporter	-0.59	0.21
	AN0418	Putative high-affinity urea/H^+ symporter	-0.58	0.08
	AN7379	Orthologue(s) have role in negative regulation of transcription from RNA polymerase II promoter, regulation of nitrogen utilization and nucleus localization	0.51	0.33
cpcA	AN3675	Transcription factor of the Gcn4p c-Jun-like type	1.02	1.53
jlbA	AN1812	bZIP transcription factor	1.3	0.04
III - Calcium signalling				
	AN3585	Transcript induced in response to calcium dichloride in a CrzA-dependent manner	1.42	3.72
pmcB	AN4920	Calcium-transporting mitochondrial ATPase involved in calcium homeostasis	1.42	1.66
	AN3998	Transcript induced in response to calcium dichloride in a CrzA-dependent manner	1.26	1.01
	AN3420	Transcript induced in response to calcium dichloride in a CrzA-dependent manner	1.05	1.17
	AN4418	Transcript induced in response to calcium dichloride in a CrzA-	1.03	-0.03

		dependent manner		
	AN2427	Transcript induced in response to calcium dichloride in a CrzA-dependent manner	1.00	1.07
	AN0419	Transcript induced in response to calcium dichloride in a CrzA-dependent manner	0.88	-0.99
	AN3751	Transcript induced in response to calcium dichloride in a CrzA-dependent manner	0.86	3.56
	AN5372	Transcript induced in response to calcium dichloride in a CrzA-dependent manner	0.82	-0.84
	AN5993	Has domain(s) with predicted calcium binding activity	0.76	8.08
	AN5341	Orthologue(s) have calcium binding activity	0.74	-0.33
	AN2826	Transcript induced in response to calcium dichloride in a CrzA-dependent manner	0.73	2.12
	AN1950	Orthologue(s) have FAD *trans*-membrane transporter activity, calcium channel activity	0.72	-0.26
	AN5302	Transcript induced in response to calcium dichloride in a CrzA-dependent manner	0.64	1.14
mid1	AN8842	Stretch-activated calcium channel	0.63	-0.01
pmrA	AN7464	Calcium-transporting ATPase with a predicted role in energy metabolism	-0.74	-0.67
	AN8774	Transcript induced in response to calcium dichloride in a CrzA-dependent manner	0.55	1.26
IV - Development				
	AN4674	Orthologue(s) have role in asexual sporulation	1.14	0.28
mstC	AN6669	High-affinity glucose transporter active in germinating conidia	0.92	1.48
	AN0928	Orthologue(s) have role in conidiophore development	0.90	0.00
	AN5619	Orthologue(s) have metallopeptidase activity, role in ascospore development	0.88	0.37

fbx15	AN2505	F-box protein	0.88	1.25
	AN2856	Orthologue(s) have 3'-5' exonuclease activity, role in ascospore formation, fruiting body development, pre-miRNA processing and perinuclear region of cytoplasm localization	0.80	1.50
	AN3689	Orthologue(s) have role in ascospore formation	0.69	0.79
esdC	AN9121	Protein with a glycogen binding domain involved in sexual development	0.68	0.76
	AN6898	Orthologue(s) have role in asexual sporulation	0.65	-0.27
	AN1131	Putative cytosolic Cu/Zn superoxide dismutase	0.63	0.17
	AN3813	Orthologue(s) have copper uptake *trans*-membrane transporter activity and role in aerobic respiration	0.58	-1.80
MAT1	AN2755	Alpha-domain mating-type protein	0.52	0.29
fcyB	AN10767	Purine-cytosine transporter	-0.58	Not detectable
tmpA	AN0055	*Trans*-membrane protein involved in regulation of conidium development	-0.58	-3.11
fluG	AN4819	Cytoplasmic protein involved in regulation of conidiation and sterigmatocystin production	-0.66	0.43
cffA	AN5844	Orthologue of *Neurospora crassa conF*, light-induced transcript expressed during conidiation in *N. crassa*	-0.71	1.41
gsk3	AN6508	Protein kinase	-0.80	-0.62
rasA	AN0182	Small monomeric GTPase of the Ras superfamily involved in regulation of development	-0.81	-0.47
V – Secondary metabolite gene cluster				
***ors* gene cluster**				
orsA	AN7909	Polyketide synthase	1.57	6.91
orsB	AN7911	Putative amidohydrolase	2.32	7.91
orsC	AN7912	Putative tyrosinase	2.28	4.41
orsD	AN7913	Protein of unknown function	2.64	4.53

orsE	AN7914	Putative alcohol dehydrogenase	1.58	5.85
***atn* gene cluster**				
atnK	AN7875	Protein of unknown function	1.09	2.08
atnI	AN7877	RTA-like protein	0.87	0.46
atnB	AN7883	YCII-related domain	1.04	6.90
***dba* gene cluster**				
cipB	AN7895	Putative oxidoreductase	0.89	3.86
dbaA	AN7896	$Zn(II)_2Cys_6$ transcription factor	0.77	6.33
dbaB	AN7897	FAD-binding monooxygenase	0.80	9.96
Cichorine gene cluster				
	AN6437	Orthologue of *Aspergillus versicolor* Aspve1_0052718 and *Aspergillus sydowii* Aspsy1_0031878	1.04	-0.39
	AN6440	Orthologue of *Aspergillus versicolor* Aspve1_0168042, *Aspergillus sydowii* Aspsy1_0031884	0.76	3.85
	AN6441	Protein of unknown function	0.77	2.80
cicE	AN6447	Predicted O-methyltransferase	0.62	0.18
***stc* gene cluster**				
stcO	AN7811	Sterigmatocystin biosynthesis protein	0.58	-0.95
stcI	AN7816	Putative lipase/esterase	0.59	0.28
stcE	AN7821	Norsolorinic acid reductase	0.48	0.56
***mdp* gene cluster**				
mdpD	AN0147	Flavin-containing monooxygenase	0.57	0.19
***eas* gene cluster**				
easC	AN2548	Acyltransferase	-0.58	-3.83
easD	AN2549	Acyl-CoA ligase	-1.07	-4.39
VII – Transcriptional regulators				
	AN0585	Has domain(s) with predicted RNA polymerase II transcription factor activity	-0.69	-3.12
jlbA	AN1812	bZIP transcription factor	1.28	0.04
	AN2672	Has domain(s) with predicted DNA binding activity	0.81	0.19
	AN2839	Has domain(s) with predicted DNA binding activity	-0.48	0.40
sltA	AN2919	C2H2 zinc-finger transcription factor	0.81	0.13

tamA	AN2944	Transcriptional co-activator of the major nitrogen regulatory protein AreA	-0.80	-0.35
	AN3120	Has domain(s) with predicted DNA binding activity	0.63	-0.62
	AN3356	Has domain(s) with predicted DNA binding activity	0.87	1.07
	AN3433	Has domain(s) with predicted RNA polymerase II transcription factor activity	1.61	3.08
cpcA	AN3675	Transcription factor of the Gcn4p c-Jun-like type	1.02	1.53
	AN4324	Has domain(s) with predicted DNA binding activity	1.41	0.08
	AN5052	Has domain(s) with predicted DNA binding activity	-0.81	0.32
	AN6430	Putative transcription factor with predicted role in secondary metabolite production	1.03	0.83
basR	AN7174	Has domain(s) with predicted DNA binding activity, chromatin binding activity, similarity to yeast Bas1p	0.64	5.85
	AN7765	Has domain(s) with predicted DNA binding activity	0.73	0.34
dbaA	AN7896	$Zn(II)_2Cys_6$ transcription factor with a role in secondary metabolite biosynthesis	0.77	6.33
	AN8529	Has domain(s) with predicted RNA polymerase II transcription factor activity	0.49	0.20
zipB	AN8772	Putative bZIP transcription factor	2.12	4.11
	AN9373	Has domain(s) with predicted RNA polymerase II transcription factor activity	1.22	0.45
	AN11165	Has domain(s) with predicted RNA polymerase II transcription factor activity	0.70	Not detectable
zipA	AN11891	Putative bZIP transcription factor	1.04	Not detectable
	AN13001	Has domain(s) with predicted RNA polymerase II transcription factor activity	0.69	Not detectable

328

329 **Table S4.** List of strains used in this study.

Strain	Genotype	Reference
Aspergillus nidulans		
FGSC A1153	*yA1*, *pabaA1*; *argB2*; *pyroA4*, *nkuA::bar*	(19)
A1153Δ*gcnE*	*yA1, pabaA1; gcnE::argB2; pyroA4, nkuA::bar*	(17)
A1153Δ*basR*	*yA1, pabaA1; basR::argB2; pyroA4, nkuA::bar*	This study
A1153*tet*^{On}-*basR*	*yA1, pabaA1; argB2::pabaA1-tet*^{On}-*basR; pyroA4, nkuA::bar*	This study
Aspergillus sydowii		
CBS 593.65		Westerdijk Fungal Bio Diversity Institute, Netherlands
tet^{On}-*basR*	Ectopic integration of pUC18 *tet*^{ON}-*basR-hph*	This study
***Streptomyces* spp.**		
Streptomyces rapamycinicus ATCC 29253		(20)
Streptomyces lividans TK24		(21)

330

331 **Table S5.** List of primers used in this study.

Name	**Sequence (5'- 3')**
For generation of constructs for transformation of *A. nidulans*	
argB2for	ATGGGAGTCAAAGTTCTGTTTGC
argB2rev	GGAAGCGAGAGAACATGTCAA
basAlbfor	GCAGATCCAATGCCAGATGC
basAArgBlbrev	AACAGAACTTTGACTCCCATTATGAGGAGAAGATGATTATC
basAArgBrbfor	GACATGTTCTCTCGCTTCCGATTACTGTGATTATTGGCAGC
basArbrev	AGTTAAACATCAAGGACTTGGG
NJ08	TGCCAGGGATAGAAACATGT
NJ09	CGCAGACCTTTCTACAGATCTGGCATATGAGGAGAAGATGATTATC
NJ10	TCCGGTTTCATACACCGGGCAAAGAATCTGGACATGCGACGGAG
NJ11	TCCATCTCAACTCCATCACATCACAATGACAGAACCTCGCCGG
NJ12	TACCTATGTCTAGTAAAAGGAT
NJ41	TTTACGGTGCACATGTTTCTATCCCTGGCACACNNNGTGTAGAAGATCTCCTAC AATATTCTCAGC
NJ42	CAAGAGCTATCCTTTTACTAGACATAGGTAAACTCGAGCCATCCGGAT
NJ102	GCAGCTGAGAATATTGTAGGAGATCTTCTAACGCGTAGTTGCATCCATTTTCTC ACTG
NJ103	GATCAGGGCAAACAGAACTTTGACTCCCATGGCCTGGTGAGTTGCTTAT
NJ104	AATAACTAATTGACATGTTCTCTCGCTTCCCGGCTCCATTTGTGACTGG
NJ105	AACACCATATCCATCCGGATGGCTCGAGTTACGCGTTGATTGTTGTGTTGTTTT GAAGC
NJ106	AACTCGAGCCATCCGGAT
NJ106	TAGAAGATCTCCTACAATATTCTCAGC
Pabacassfor	TGCCAGATCTGTAGAAAGGTC
TetONfor	TCTTTGCCCGGTGTATGAAACC

Name	Sequence (5'- 3')
TetONrev	TGTGATGTGATGGAGTTGAGATGG
TetON_pUC18tailF	CACGACGTTGTAAAACGACGGCCAGTGCCATCTTTGCCCGGTGTATGAAA
Asyd_basRF	ATGGCTGAACAACGTCGGCG
Asyd_basRR	TCAATATCCATACGACTGCC
poliC_basRsidtai	AGTTGTCCAGCGCCGACGTTGTTCAGCCATTGTGATGTGATGGAGTTGAG
Ttef_sydbastail_	CTCCAGAGAGGGCAGTCGTATGGATATTGAGCGGACATTCGATTTATGCC
hph_puc18tail_R	GATCCTCTAGAGTCGACCTGCAGGCATGCACTATTCCTTTGCCCTCGGAC
qRT-PCR	
Qacnfwd	CACCCTTGTTCTTGTTTTGCTC
Qacnrev	AAGTTCGCTTTGGCAACGC
qorsAfor	CTATACCACCGATAGCCAGGAC
qorsArev	CAGTGAGCAGGGCAAAGAAG
qorsDfor	GCAACGAGCCTGACATTACC
qorsDrev	CCGCACATCAACCATCTCTG
qareAfor	AAATCTAGCTCAGCGGCGAC
qareArev	GGGCTTTCCGCCATATCAAC
qniaDfor	CTGACGAAGGGGAGTGAAAG
qniaDrev	TCCATCCCAACGACAGTAGG
qprnDfor	CGCTTTTGGTCTGCGTTAC
qprnDrev	CCGCTCAAAAACCAGACAATC
qgdhAfor	TCAAGGGCATCATGGAGGAC
qgdhArev	CTTGGTGAAACCGGCAATG

Name	Sequence (5'- 3')
qniiAfor	GCGGGAAGATGGCTGGATTTAC
qniiArev	CCACAGCTTCACCCTTCTTCAC
qtamAfor	TGATGACCAGCTCGTCAAAACC
qtamrev	CCGCATCGTGCATACTTTCCTC
qgltAfor	GCCCGTAAGAATGTCAAGACCC
qgltArev	GCTGAGAGCTGATGCCAGAAAG
qmeaAfor	TGACTACCTTGCCTGGACAC
qmeaArev	GCCGTTGCGATTCTTCCTTG
qureDfor	AGCGGGATGCAGCAAAGATG
qureDrev	AAGGCTCAACACTCCCAGAC
qprnBfor	GTCAGAGGTTGACATCTTTACG
qprnBrev	AAATCCACCACCAGACTCG
qbasRfw	GCGGGTACATGCCACAATAC
qbasRrev	TCTCGGGCATCATCAACTCC

Additional data table S1. (separate file)

Summary of DCS analysis of H3K9ac between *A. nidulans* monoculture and co-cultivation with *S. rapamycinicus*. Significantly higher acetylated genes are marked in red and lower acetylated genes are marked in blue.

Additional data table S3. (separate file)

Summary of ChIP-seq data.

341 **References**

342 1. Boedi S, Reyes-Dominguez Y, & Strauss J (2012) Chromatin immunoprecipitation
343 analysis in filamentous fungi. *Fungal secondary metabolism: methods and protocols*,
344 eds Keller NP & Turner G (Humana Press, Totowa, NJ), pp 221-236.
345 2. Cerqueira GC*, et al.* (2014) The Aspergillus Genome Database: multispecies curation
346 and incorporation of RNA-Seq data to improve structural gene annotations. *Nucleic*
347 *Acids Research* 42(Database issue):D705-D710.
348 3. Gel B*, et al.* (2016) regioneR: an R/Bioconductor package for the association analysis
349 of genomic regions based on permutation tests. *Bioinformatics* 32(2):289-291.
350 4. Robinson MD & Oshlack A (2010) A scaling normalization method for differential
351 expression analysis of RNA-seq data. *Genome Biol.* 11(3):R25.
352 5. Zhang Y*, et al.* (2008) Model-based Analysis of ChIP-Seq (MACS). *Genome Biol.*
353 9(9):R137-R137.
354 6. Thorvaldsdóttir H, Robinson JT, & Mesirov JP (2013) Integrative genomics viewer
355 (IGV): high-performance genomics data visualization and exploration. *Briefings Bioinf.*
356 14(2):178-192.
357 7. Szewczyk E*, et al.* (2007) Fusion PCR and gene targeting in *Aspergillus nidulans*. *Nat.*
358 *Protoc.* 1(6):3111-3120.
359 8. Schroeckh V*, et al.* (2009) Intimate bacterial-fungal interaction triggers biosynthesis
360 of archetypal polyketides in *Aspergillus nidulans*. *PNAS* 106(34):14558-14563.
361 9. Ballance DJ & Turner G (1985) Development of a high-frequency transforming vector
362 for *Aspergillus nidulans*. *Gene* 36(3):321-331.
363 10. Helmschrott C, Sasse A, Samantaray S, Krappmann S, & Wagener J (2013) Upgrading
364 fungal gene expression on demand: improved systems for doxycycline-dependent
365 silencing in *Aspergillus fumigatus*. *Appl. Environ. Microbiol.* 79(5):1751-1754.
366 11. Docimo T*, et al.* (2012) The first step in the biosynthesis of cocaine in *Erythroxylum*
367 *coca*: the characterization of arginine and ornithine decarboxylases. *Plant Mol. Biol.*
368 78(6):599-615.
369 12. Jakimowicz D*, et al.* (1998) Structural elements of the *Streptomyces oriC* region and
370 their interactions with the DnaA protein. *Microbiology* 144(5):1281-1290.
371 13. Ekblom R & Wolf JBW (2014) A field guide to whole-genome sequencing, assembly
372 and annotation. *Evol. Appl.* 7(9):1026-1042.
373 14. Yu G, Wang L-G, & He Q-Y (2015) ChIPseeker: an R/Bioconductor package for ChIP
374 peak annotation, comparison and visualization. *Bioinformatics* 31(14):2382-2383.
375 15. Kaplan N*, et al.* (2010) Nucleosome sequence preferences influence in vivo
376 nucleosome organization. *Nat. Struct. Mol. Biol.* 17(8):918-922.
377 16. Gacek A & Strauss J (2012) The chromatin code of fungal secondary metabolite gene
378 clusters. *Appl. Microbiol. Biotechnol.* 95(6):1389-1404.
379 17. Nützmann H-W*, et al.* (2011) Bacteria-induced natural product formation in the
380 fungus *Aspergillus nidulans* requires Saga/Ada-mediated histone acetylation. *PNAS*
381 108(34):14282-14287.
382 18. Priebe S, Kreisel C, Horn F, Guthke R, & Linde J (2015) FungiFun2: A comprehensive
383 online resource for systematic analysis of gene lists from fungal species.
384 *Bioinformatics* 31(3):445-446.

385 19. Nayak T*, et al.* (2006) A versatile and efficient gene-targeting system for *Aspergillus*
386 *nidulans*. *Genetics* 172(3):1557-1566.
387 20. Kumar Y & Goodfellow M (2008) Five new members of the *Streptomyces*
388 *violaceusniger* 16S rRNA gene clade: *Streptomyces castelarensis* sp. nov., comb. nov.,
389 *Streptomyces himastatinicus* sp. nov., *Streptomyces mordarskii* sp. nov.,
390 *Streptomyces rapamycinicus* sp. nov. and *Streptomyces ruanii* sp. nov. *Int. J. Syst.*
391 *Evol. Microbiol.* 58(Pt 6):1369-1378.
392 21. Kieser T, Bibb MJ, Buttner MJ, Chater KF, & Hopwood DA (2000) *Practical*
393 *Streptomyes genetics* (John Innes Foundation, Norwich, United Kingdom).

394